



# RESEARCH MEMORANDUM

AN EXPERIMENTAL STUDY AT MODERATE AND HIGH SUBSONIC  
SPEEDS OF THE FLOW OVER WINGS WITH  $30^\circ$  AND  $45^\circ$  OF  
SWEEPFORWARD IN CONJUNCTION WITH A FUSELAGE

By Richard T. Whitcomb

Langley Aeronautical Laboratory  
Langley Field, Va.

NATIONAL ADVISORY COMMITTEE  
FOR AERONAUTICS

WASHINGTON

June 15, 1951

## NATIONAL ADVISORY COMMITTEE FOR AERONAUTICS

## RESEARCH MEMORANDUM

AN EXPERIMENTAL STUDY AT MODERATE AND HIGH SUBSONIC  
SPEEDS OF THE FLOW OVER WINGS WITH  $30^\circ$  AND  $45^\circ$  OF  
SWEEPFORWARD IN CONJUNCTION WITH A FUSELAGE

By Richard T. Whitcomb

## SUMMARY

Pressure distributions and wake measurements have been obtained for wings with  $30^\circ$  and  $45^\circ$  of sweepforward, in conjunction with a mid-wing fuselage, at Mach numbers to 0.96. The wings had an NACA 65-210 section, a taper ratio of 0.38, and aspect ratios of 7.5 and 5.2. A study of the results of these measurements indicates that severe negative pressure-coefficient peaks develop on the leading edge of the upper surface of the sweptforward wings near the wing-fuselage juncture, even for low angles of attack at a Mach number of 0.60. As the angle of attack was increased, severe separation developed initially in this region. Shocks and associated separation occurred initially near the wing-fuselage juncture of the sweptforward wings at Mach numbers below the drag-divergence values. At Mach numbers above the drag-divergence values, the separation on this region of the wing with  $30^\circ$  of sweepforward was more severe than that on the same wing with no sweep for the same Mach numbers and angles of attack. No loss in section normal-force coefficient was associated with this separation. The separation, associated with the onset of shock on the upper surface of the mid-semispan and outboard regions of the wing with  $30^\circ$  of sweepforward, was considerably less severe than that on the corresponding regions of the same wing with  $30^\circ$  of sweepback at the same Mach numbers and angles of attack.

## INTRODUCTION

To provide a basis for a further understanding of the flow over unswept and swept wings at moderate and high subsonic speeds, pressure, tuft, and wake measurements have been made on and behind a high-aspect-ratio tapered wing with no sweep and  $30^\circ$  and  $45^\circ$  of sweepback and sweepforward, in conjunction with a typical fuselage. These measurements were

made in the Langley 8-foot high-speed tunnel at Mach numbers from 0.6 to 0.96. A study of the measurements made for the sweptforward wings is presented herein. Similar studies for the unswept and swept-back wings are presented in references 1 and 2, respectively.

### SYMBOLS

b	span of model
d	sweptforward semispan, distance between intersections of quarter-chord line (chord perpendicular to this line) with root and tip chords parallel with air stream
s	distance measured along quarter-chord line from plane of symmetry
$c_{\Delta}$	section chord perpendicular to quarter-chord line
$\bar{c}_w$	mean aerodynamic chord, inches
l	distance from leading edge of wing perpendicular to quarter chord
$\Lambda$	sweep angle between line perpendicular to plane of symmetry and quarter-chord line
$\alpha$	geometric angle of attack
M	Mach number
q	dynamic pressure in undisturbed stream, pounds per square foot $\left(\frac{1}{2}\rho V^2\right)$
V	velocity in undisturbed stream, feet per second
$\rho$	mass density in undisturbed stream, slugs per cubic foot
p	local static pressure at a point on airfoil or fuselage, pounds per square foot
$P_0$	static pressure in undisturbed stream, pounds per square foot

P pressure coefficient  $\left(\frac{p - p_0}{q}\right)$

$c_n$  wing-section normal-force coefficient (section perpendicular

to quarter-chord line  $\left(\frac{1}{c_A} \int_0^{c_A} (P_L - P_U) dz\right)$

$c_{d_0}$  wing-section profile-drag coefficient from wake-survey measurements based on local stream direction

$\Delta H$  total-pressure loss, pounds per square foot

Subscripts:

U upper surface

L lower surface

cr critical.

## APPARATUS

Wing models.- The models tested to obtain the results for the unswept wing as described in reference 1 were also used to obtain the data for the sweptforward configurations as presented herein.

For the unswept condition, the wings investigated had an NACA 65-210 section, an aspect ratio of 9.0, and a taper ratio of 0.4 with no twist or dihedral. The models were supported in the tunnel by means of the vertical steel plate which is completely described in reference 3. Swept configurations were obtained by rotating the complete wings with respect to the fixed support plate. Wall-pressure measurements indicated that the flow over the model on one side of the plate had very little effect on the flow on the other side even at the highest test Mach numbers. A given configuration represents, therefore, not a yawed model but half a sweptback model and half a sweptforward model. Revised tips were added to each configuration. Plan forms and basic dimensions of the configurations with  $30^\circ$  and  $45^\circ$  of sweepforward are presented in figure 1. The taper ratios of the configurations were 0.38; the aspect ratios were 7.5 and 5.2. Other dimensions are given in table I of reference 4.

Two wing models were used in the investigation. One, used to obtain the static-pressure data, incorporated 20 static-pressure orifices at each of eight stations along the wing semispan in lines perpendicular to the quarter-chord line. A 20-percent-chord straight-sided aileron, as shown in figure 1, was incorporated in this model. The aileron deflection was  $0^\circ$  for the investigation described herein. The second wing model, used for the wake and tuft measurements incorporated no pressure orifices or aileron.

Fuselage.- The midwing fuselage was simulated by the addition of two half bodies of revolution to the test configuration at the surfaces of the support plate. The dimensions of the half bodies of revolution are shown in figure 1. Twenty-eight pressure orifices were placed in one of the halves of the fuselage in two planes at  $45^\circ$  to the plane of symmetry through the center line as shown in figure 1.

Survey apparatus.- Total- and static-pressure measurements were made in planes parallel to the plane of symmetry at various stations behind the wing by means of the rake shown with the unswept configuration in figure 2 and described in reference 3.

Reynolds numbers.- The variations of Reynolds number with Mach number for the configurations with the two sweptforward wings are presented in figure 3. The Reynolds numbers are based on the mean aerodynamic chords of the wings outboard of the fuselage.

## RESULTS

Pressure distributions.- The distributions of pressure on the wings with  $30^\circ$  and  $45^\circ$  of sweepforward for a number of test conditions are presented in figures 4 and 5, respectively. Other pressure data obtained during the investigation are presented in reference 5. The distributions are presented in the form of contours of equal pressure coefficient on plan forms of the wing. The positions of chordwise pressure peaks are indicated by lines of short dashes. The locations of the rows of pressure orifices and the tenths of chords of the various stations are indicated by light lines of long dashes. To indicate more explicitly the changes in pressure on the wings near the wing-fuselage juncture, pressure distributions in the stream direction at a station 0.25-fuselage radius from the surface of the fuselage obtained from the pressure contours are presented in figures 6 and 7. Pressure distributions obtained at the two streamwise rows of orifices on the surface of the fuselage are also presented in figures 6 and 7. Spanwise variations in wing-section normal-force coefficient,  $c_n'$ , on the wings with  $30^\circ$  and  $45^\circ$  sweepforward

are presented in figures 8 and 9. The coefficients presented are for sections perpendicular to the quarter-chord line of the unswept wing.

Wake measurements.- Some of the distributions of total-pressure loss in planes parallel with the plane of symmetry at the various measurement stations behind the wing with  $30^\circ$  of sweepforward are presented in figure 10. The locations of the wake-measurement stations are indicated in figure 1. The spanwise variations of wing-section profile-drag coefficient at various Mach numbers for the wing with  $30^\circ$  of sweepforward at various angles of attack are presented in figure 11. These coefficients were obtained from total-pressure measurements by using the method described in reference 6.

Because of the pronounced spanwise pressure gradients, the low-energy air of the boundary layer moves inward along the aft portion of the sweptforward wings. As a result of this movement, the wake measurements do not indicate exactly the spanwise locations of the sources of the low-energy air crossing the plane of measurement. Also, because of this flow, part of the low-energy air associated with wing losses crosses the plane of measurement above or below the fuselage. As a result, the wake measurements made behind the wing do not indicate all the losses produced by the wings. The effects of this spanwise flow on the qualitative indications of the wake measurement are believed to be small for the wing with  $30^\circ$  of sweepforward at low angles of attack. However, for this wing at higher angles of attack, the spanwise flow may be severe enough to make the indications of the wake measurements somewhat unreliable. The effect of the spanwise flow of low-energy air on the accuracy of the indications of the wake measurements for the wing with  $45^\circ$  of sweepforward are undoubtedly considerable especially at the higher angles of attack. Therefore, none of the wake data measured behind this wing are presented.

No tuft patterns were obtained for these sweptforward wings as they were for the comparable sweptback wings (reference 2).

Corrections.- No corrections for the effects of tunnel-wall interference have been applied to the data presented. Estimations of the order of magnitude of these effects indicate that the corrections to be applied to dynamic pressures and Mach numbers for all conditions are less than 1 percent. Only data relatively free from choking effects have been used in this study. A discussion of the limitations imposed by blockage near choking during the investigation is presented in reference 3. The results of calculations of the bending of the wing produced by the air loads on the structure, similar to those described in reference 7, indicate that this bending results in tip washin for all conditions. The maximum increases of the aerodynamic angles of attack, at a Mach number of 0.96 for the wing with  $45^\circ$  of sweepback,

are approximately 10 percent of the mean aerodynamic angles of attack for the wing. Such increases should not generally result in significant changes in the flow phenomena discussed herein.

## DISCUSSION

Obviously, because of the beneficial effects of sweep, the general over-all characteristics of the wings with different amounts of sweep-forward differ markedly at a given high subsonic Mach number (fig. 12). In this discussion, comparisons have been made for the Mach numbers at which the general over-all drag characteristics for the wings are approximately the same.

### Angle of Attack of $2^\circ$ at a Mach Number of 0.60

Pressure distributions.- The pressure contours (figs. 4(a) and 5(a)) indicate the presence of negative pressure peaks on the leading edges of the upper surfaces of the sweptforward wings near the junctures for an angle of attack of  $2^\circ$  at a Mach number of 0.60. For the wing with  $30^\circ$  of sweepforward the maximum negative pressures in this region are greater than those on the same region of the unswept wing for the same condition (fig. 13(a)). A comparison of these results with data obtained for a similar sweptforward wing without a fuselage (reference 8) indicates that these peaks are due primarily to the induced flow peculiar to sweptforward wings. The peaks are also due in part to the mutual interference of the wing and fuselage, which caused the lesser peaks on the same regions of the comparable unswept and sweptback wings (references 1 and 2).

Profile drag.- The profile-drag coefficients for the various sections of the wing with  $30^\circ$  of sweepforward at  $2^\circ$  angle of attack for a Mach number of 0.60 (fig. 11) are generally less than those for the unswept wing at the same condition (reference 1). As a result, the wing-profile drag coefficient for the sweptforward wing is less than that for the unswept wing as is the coefficient for the comparable sweptback wing (fig. 12) (reference 2). The differences can be attributed to the same factors which caused the similar reduction for the sweptback wings; reductions in the local induced velocities, an increase in the extent of the laminar boundary layer, and possibly other factors.

### Angle of Attack of $2^\circ$ at Mach Numbers Slightly Below the Drag-Divergence Values

The Mach numbers at which the over-all characteristics of the wings with  $30^\circ$  and  $45^\circ$  of sweepforward change markedly, the drag-divergence

Mach numbers, are approximately 0.84 and 0.94, respectively, for  $2^\circ$  angle of attack (fig. 12). At Mach numbers somewhat below these values, local but significant changes in the flow phenomena occur on the inboard sections of the sweptforward wings. These changes are indicated by the data obtained at Mach numbers of 0.80 and 0.89 for the wings with  $30^\circ$  and  $45^\circ$  of sweepforward, respectively.

Pressure distributions.- When the Mach number is increased from 0.60 to 0.80 and 0.89 for  $30^\circ$  and  $45^\circ$  of sweepforward, respectively, for  $2^\circ$  angle of attack, the regions of high induced velocities present on the leading edges of the upper surfaces of the sections near the wing-fuselage junctures spread rearward (figs. 4(a), 4(b), 5(a), and 5(b)). This change can be attributed primarily to the presence of local supersonic velocities near the wing-fuselage junctures.

Shocks.- When the Mach number is increased to 0.80 and 0.89 for the wings with  $30^\circ$  and  $45^\circ$  sweepforward, respectively, at  $2^\circ$  angle of attack, the maximum local Mach numbers on the upper surface of the sections near the wing-fuselage junctures reach values of 1.24 and 1.27. The pressure contours (figs. 4(b) and 5(b)) and wake measurements (fig. 10(a)) indicate that perceptible shocks are associated with the presence of these local supersonic velocities. The presence of these shocks is indicated by a relatively extensive region of low total pressure losses above the boundary-layer wakes. These shocks are apparently nearly normal to the fuselage and extend from about the 25-percent-chord station of the wing-fuselage junctures to approximately the 50-percent-chord stations of the quarter semispan sections. The shocks are strongest at the junctures, as would be expected.

Separation.- The wake measurements (fig. 10 and unpublished data) indicate the presence of moderate separation, because of the local shocks, on the inboard sections at the conditions under consideration. This separation is believed to be accentuated by the inflow of the low-energy boundary-layer air from sections farther outboard onto these inboard sections associated with the spanwise pressure gradients (reference 9).

An interpolation between the available wake data indicates that perceptible separation occurred initially on the inboard sections of the wing with  $30^\circ$  of sweepforward at a Mach number of approximately 0.75 (fig. 11). This value is about the same as the value at which separation occurred initially on the unswept wing (fig. 12). However, because the separation is localized, the resulting increase in the wing-profile drag coefficient with Mach number for the wings with  $30^\circ$  of sweepforward is slight below a Mach number of 0.84 (fig. 11 of reference 8).



Angle of Attack of  $2^\circ$  at Mach Numbers  
Greater Than the Drag-Divergence Values

Pressure distributions.- When the Mach numbers are increased beyond the drag-divergence values of approximately 0.84 and 0.94 for the wings with  $30^\circ$  and  $45^\circ$  of sweepforward, respectively, the regions of supersonic flow present above the upper surfaces of the sections near the wing-fuselage juncture at lower speeds expand chordwise and spanwise (figs. 4 to 7). As at lower speeds, the maximum local Mach numbers in these regions for these conditions are greater than those on the unswept wing for the same Mach numbers and angles of attack (fig. 13(b)).

The chordwise pressure distributions on the midchord regions of these wings change in a manner similar to that for the comparable unswept and sweptback wings at supercritical Mach numbers (figs. 13 and 14). The changes in the distributions on the outboard sections are approximately the same as those on sections farther inboard; whereas, for the comparable unswept and sweptback wings the changes for these sections were considerably different from those for sections farther inboard.

When the Mach number is increased beyond the drag-divergence value for the wing with  $30^\circ$  of sweepforward, the relative changes in the normal-force coefficients of sections near the wing-fuselage juncture are no greater than those of sections farther outboard (fig. 8), in spite of the severe increase in separation on these inboard sections.

Shocks.- The pressure contours (figs. 4 and 5) and wake measurements (fig. 10) indicate that the shocks which formed above the wings near the wing-fuselage junctures at lower Mach numbers increase in intensity, move rearward, and spread outward and vertically when the Mach numbers are increased beyond the drag-divergence values.

The wake measurements indicate that the normal shock above the upper surface of the inboard sections of the wing with  $30^\circ$  of sweepforward at an angle of attack of  $2^\circ$  and a Mach number of 0.89 is considerably stronger and more extensive vertically than the strongest portion of the shock on the unswept wing for the same Mach number and angle of attack (fig. 8 of reference 1). This might be expected on the basis of the higher induced velocities on this region of the swept-forward wing.

The pressure contours (fig. 4(d)) indicate the possible presence of a weak oblique shock above the midsemispan region of the wing with  $30^\circ$  of sweepforward at a Mach number of 0.89. The contours indicate that this shock merges with the nearly normal shock above the inboard sections. The wake measurements indicate that this oblique shock is considerably weaker than that present above the midsemispan region of

the same wing with  $30^\circ$  of sweepback at the same Mach number and angle of attack. The difference in shock strength is believed to be due to the greater effective sweep, as indicated by the angle of the line of peak negative pressure coefficients (figs. 4(d) and 4(b)), and the lower maximum induced velocities for this region of the sweptforward wing.

The wake and pressure measurements both indicate that no perceptible shock is present on the outboard sections of the wing with  $30^\circ$  of sweepforward at a Mach number of 0.89. The reduction of the strength of the shock on the outboard sections compared with that for the midsemispan region is due primarily to the lower maximum induced velocities on the outboard sections (figs. 4 and 5). The reduction is also believed to be a result of further increase of the effective sweep of the upper surface of the outboard sections, associated with flow around the tip due to the lift.

Separation.- When the Mach number is increased beyond the drag-divergence value, the separation associated with the nearly normal shock on the inboard region of the upper surface of the wing with  $30^\circ$  of sweepforward increases in intensity and extent (fig. 11(a)). The high section-profile drag coefficients for the juncture section, associated with this separation, is appreciably greater than the highest coefficient for the sweptback wing at the same Mach number and angle of attack; the coefficients are even greater than the highest for the unswept wing for the same condition (fig. 15).

The wake measurements indicate the presence of moderate separation on the upper surface of the sections in midsemispan region of the wing with  $30^\circ$  of sweepforward at a Mach number of 0.89. This separation is considerably less severe than that for the same region of the wing with  $30^\circ$  of sweepback at the same condition because of the weaker shock above this region of the sweptforward wing.

The data indicate no separation on the upper surface of sections near the tip of the wing with  $30^\circ$  of sweepforward at the highest test Mach numbers. For this particular Mach number and angle of attack this phenomenon is due to the lack of a shock above this region.

The increase in the drag coefficient for the entire wing with  $30^\circ$  of sweepforward is similar to that for the wing with  $30^\circ$  of sweepback, when the Mach number is increased to 0.89 (fig. 12). A major portion of the drag increase for the wing with  $30^\circ$  of sweepforward is associated with the severe losses near the juncture, whereas for the sweptback wing at similar conditions the major portion of the losses was caused by separation of the midsemispan and outboard sections (fig. 15).

### Higher Angles of Attack at a Mach Number of 0.60

Pressure distributions.- The negative pressure coefficient peaks near the leading edges of the upper surface of the sections near the junctures of the sweptforward wings with the fuselage for an angle of attack of  $7^\circ$  at a Mach number of 0.60 (figs. 4(j) and 5(f)), are considerably lower than those on sections farther outboard; however, the regions of high induced velocities near the junctures are more extensive than those on sections farther outboard. As for the comparable unswept wing at the same angle of attack and Mach number (fig. 13(c)), these changes in the pressure distribution are a result of the onset of separation in this region.

The pressures near the leading edges of the tip sections of the sweptforward wings are considerably less than those on the corresponding portions of sections farther inboard, as would be expected.

Separation.- The wake measurements (fig. 11 and unpublished data) indicate the presence of considerable separation on the upper surface of the sections of the wings near the wing-fuselage junctures at a Mach number of 0.60 and an angle of attack of  $5^\circ$ . The separation results from the relatively severe adverse pressure gradients on these sections at lower angles of attack (figs. 4(a) and 5(a)) and the marked inflow of the boundary layer to this region (reference 9).

### Higher Angles of Attack at

### High Subsonic Mach Numbers

Pressure distributions.- When the Mach number is increased to high subsonic values at  $7^\circ$  angle of attack, the peak negative pressure coefficient on the upper surface of the inboard sections of the wing with  $30^\circ$  of sweepforward increases markedly (fig. 4). This increase is believed to be a result of partial reattachment of the separated flow on the forward portion of these sections associated with the presence of local supersonic velocities. The peak coefficient on this same region of the wing with  $45^\circ$  of sweepforward remains approximately the same.

Shocks.- Wake data (fig. 10(d) and data not presented) indicate that any shocks that may be associated with the high supersonic velocities on the inboard region upper surfaces of the sweptforward wings for high subsonic Mach numbers at an angle of attack of  $5^\circ$  do not generally cause distinguishable losses in total pressure behind the wings. The apparent reductions of the shock losses are believed to be due to a reduction of the strengths of the shocks caused by the presence

of a region of severe separation and to an envelopment of the shock losses by the separation losses.

Separation.- The wake measurements (fig. 11 and data not presented) indicate that the severe separation on the sections of the sweptforward wings near the wing-fuselage junctures at a Mach number of 0.60 for high angles of attack increases markedly both in intensity and extent when the Mach number is increased to high subsonic values.

### Fuselage Pressures

As the wing is sweptforward for an angle of attack of  $2^\circ$  at a Mach number of 0.60, the peak negative pressures at the measurement station above the juncture move forward, the pressures near the leading edge of the juncture become more negative, while those near the trailing edge become more positive (figs. 6 and 7). These changes are approximately opposite to those that occur when the wing is swept back by comparable amounts (fig. 16). The peak negative pressure coefficients on the upper surface are reduced by approximately the same amount as they are when the wing is sweptback.

When the Mach number is increased to high subsonic values at  $2^\circ$  angle of attack, the peak pressure coefficients on the fuselage above the juncture first increase in magnitude and then move rearward. The increase is particularly large for the configuration with  $30^\circ$  of sweepforward. At Mach numbers higher than 0.89, the peak pressure on the upper surface of the fuselage is greater than that on the upper surface of this wing. These increases result from very pronounced expansions of the supersonic field above the inboard sections of the sweptforward wings at these Mach numbers.

The presence of the high peak negative pressure coefficients and the pronounced adverse gradients on the fuselage indicate that the very strong extensive shocks on the inboard sections of the sweptforward wings at high subsonic Mach numbers probably extend unrelieved around the fuselage.

The pressures on the lower surface of the fuselage for these configurations remain very low until the Mach number is increased to 0.89. When the Mach number is increased beyond this value, the peak pressures on this lower surface of the fuselage increase abruptly to supercritical values.

When the Mach number is increased from 0.6 to high subsonic values for the sweptforward configurations at an angle of attack of  $7^\circ$ , the peak pressure coefficients on the upper surface of the fuselage increase

only slightly in contrast to the large changes that occurred for an angle of attack of  $2^\circ$ .

### CONCLUSIONS

A study of the pressure distributions and wake measurements obtained on and behind wings with  $30^\circ$  and  $45^\circ$  of sweepforward, in conjunction with a fuselage, at moderate and high subsonic Mach numbers led to the following conclusions:

1. Severe negative pressure coefficient peaks develop on the leading edge of the upper surface of the sweptforward wings near the wing-fuselage juncture, even for low angles of attack at a Mach number of 0.60. As the angle of attack is increased, severe separation develops initially in this region.
2. Shocks and associated separation occur initially near the wing-fuselage juncture of the sweptforward wings at Mach numbers below the drag-divergence values. At Mach numbers greater than the drag-divergence values the separation on this region of the wing with  $30^\circ$  of sweepforward is more severe than that on the same wing with no sweep for the same Mach numbers and angles of attack. No loss in section normal-force coefficient is associated with this separation.
3. The separation associated with the onset of shock on the upper surface of the midsemispan and outboard regions of the wing with  $30^\circ$  of sweepforward is considerably less severe than that on the corresponding regions of the same wing with  $30^\circ$  of sweepback at the same Mach numbers and angles of attack.

Langley Aeronautical Laboratory  
National Advisory Committee for Aeronautics  
Langley Air Force Base, Va.

## REFERENCES

1. Whitcomb, Richard T.: An Experimental Study at Moderate and High Subsonic Speeds of the Flow over an Unswept Wing in Conjunction with a Fuselage. NACA RM L50L07, 1950.
2. Whitcomb, Richard T.: An Experimental Study at Moderate and High Subsonic Speeds of the Flow over Wings with  $30^\circ$  and  $45^\circ$  of Sweep-back in Conjunction with a Fuselage. NACA RM L50K27, 1950.
3. Whitcomb, Richard T.: Investigation of the Characteristics of a High-Aspect-Ratio Wing in the Langley 8-Foot High-Speed Tunnel. NACA RM L6H28a, 1946.
4. Whitcomb, Richard T.: An Investigation of the Effects of Sweep on the Characteristics of a High-Aspect-Ratio Wing in the Langley 8-Foot High-Speed Tunnel. NACA RM L6J01a, 1947.
5. Whitcomb, Richard T.: A Compilation of the Pressures Measured on a Wing and Aileron with Various Amounts of Sweep in the Langley 8-Foot High-Speed Tunnel. NACA RM L8A30a, 1948.
6. Baals, Donald D., and Mourhess, Mary J.: Numerical Evaluation of the Wake-Survey Equations for Subsonic Flow Including the Effect of Energy Addition. NACA ARR L5H27, 1945.
7. Luoma, Arvo A., Bielat, Ralph P., and Whitcomb, Richard T.: High-Speed Wind-Tunnel Investigation of the Lateral-Control Characteristics of Plain Ailerons on a Wing with Various Amounts of Sweep. NACA RM L7I15, 1947.
8. Hieser, Gerald, and Whitcomb, Charles F.: Investigation of the Effects of a Nacelle on the Aerodynamic Characteristics of a Swept Wing and the Effects of Sweep on a Wing Alone. NACA TN 1709, 1948.
9. Hieser, Gerald: Tuft Studies of the Flow over a Wing at Four Angles of Sweep. NACA RM L7C05a, 1947.

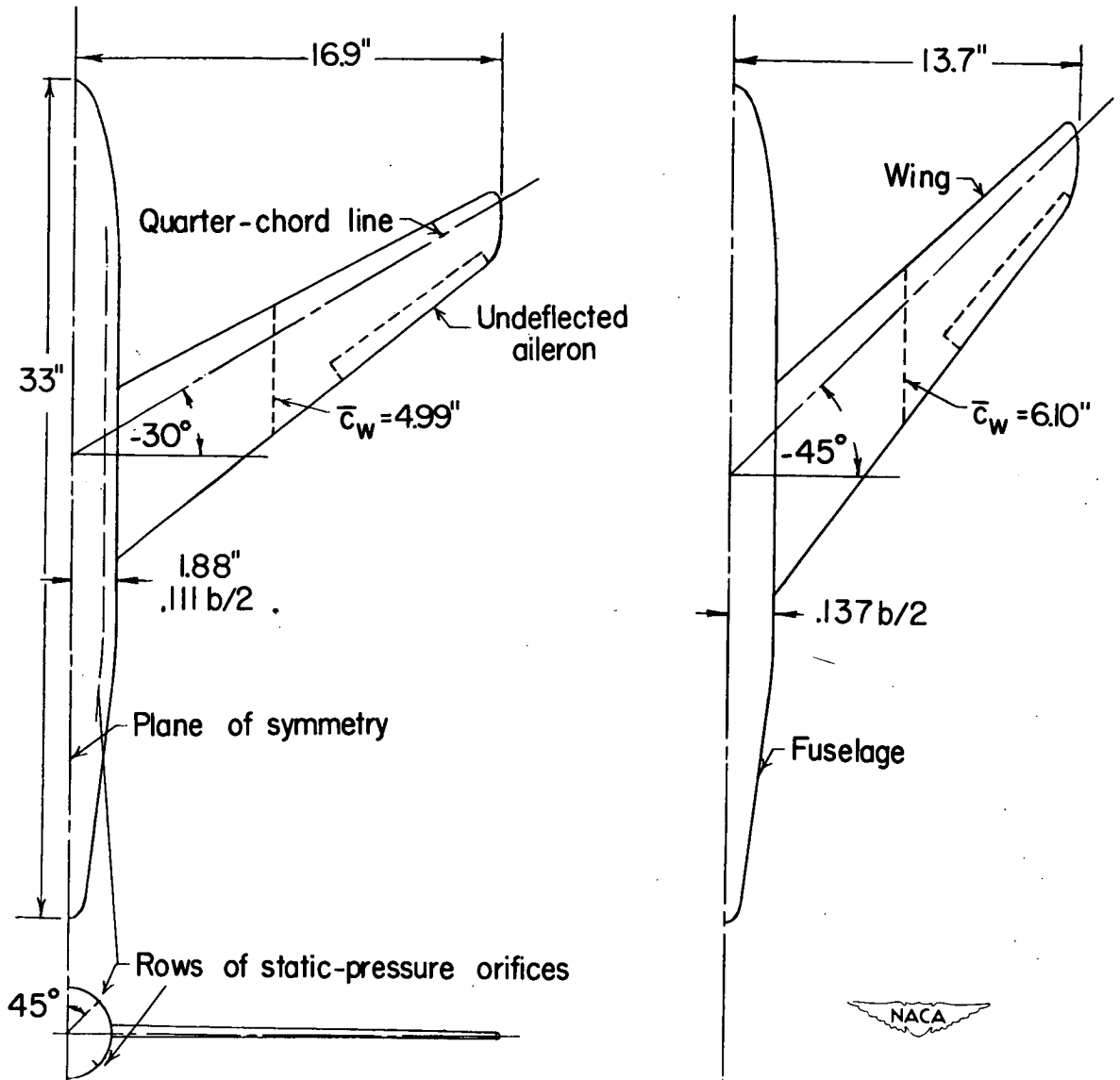


Figure 1.- Configurations.

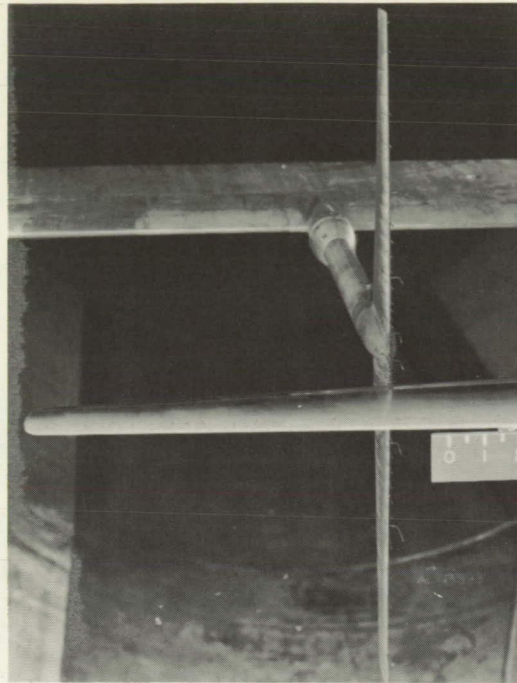


Figure 2.- Wake-survey rake.

NACA  
L-43593

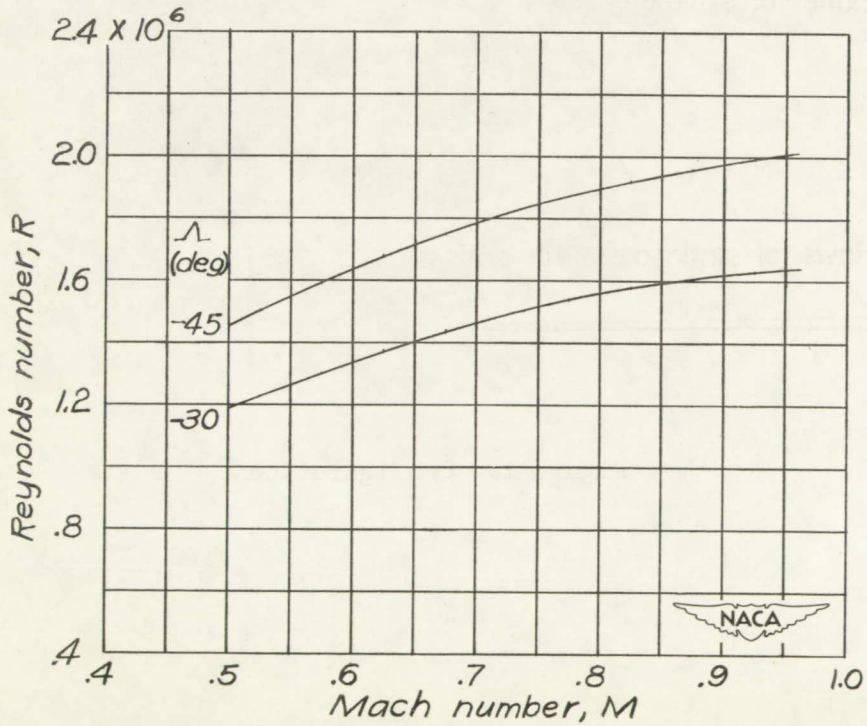


Figure 3.- Variation of Reynolds number with Mach number.



**Page intentionally left blank**

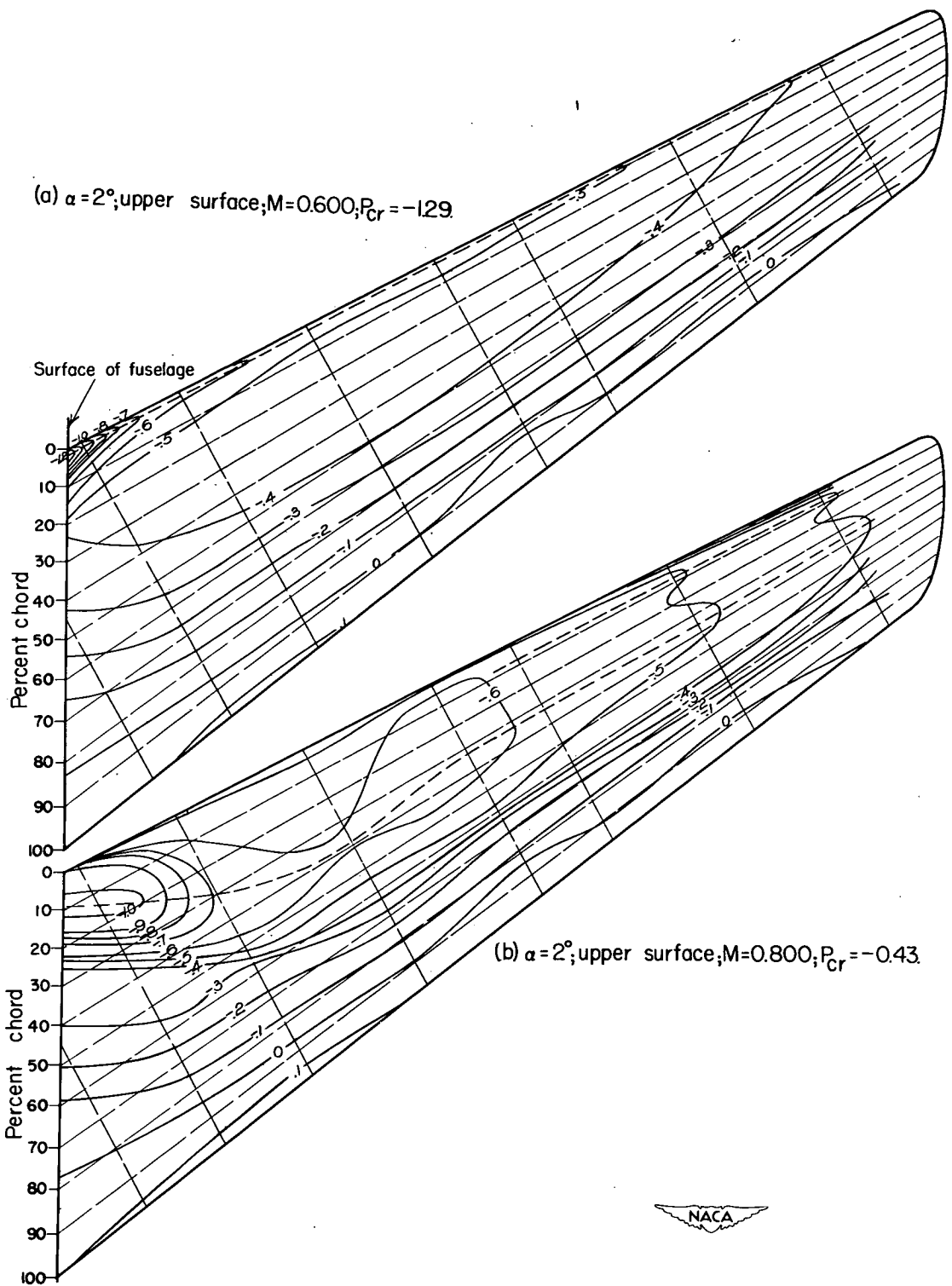
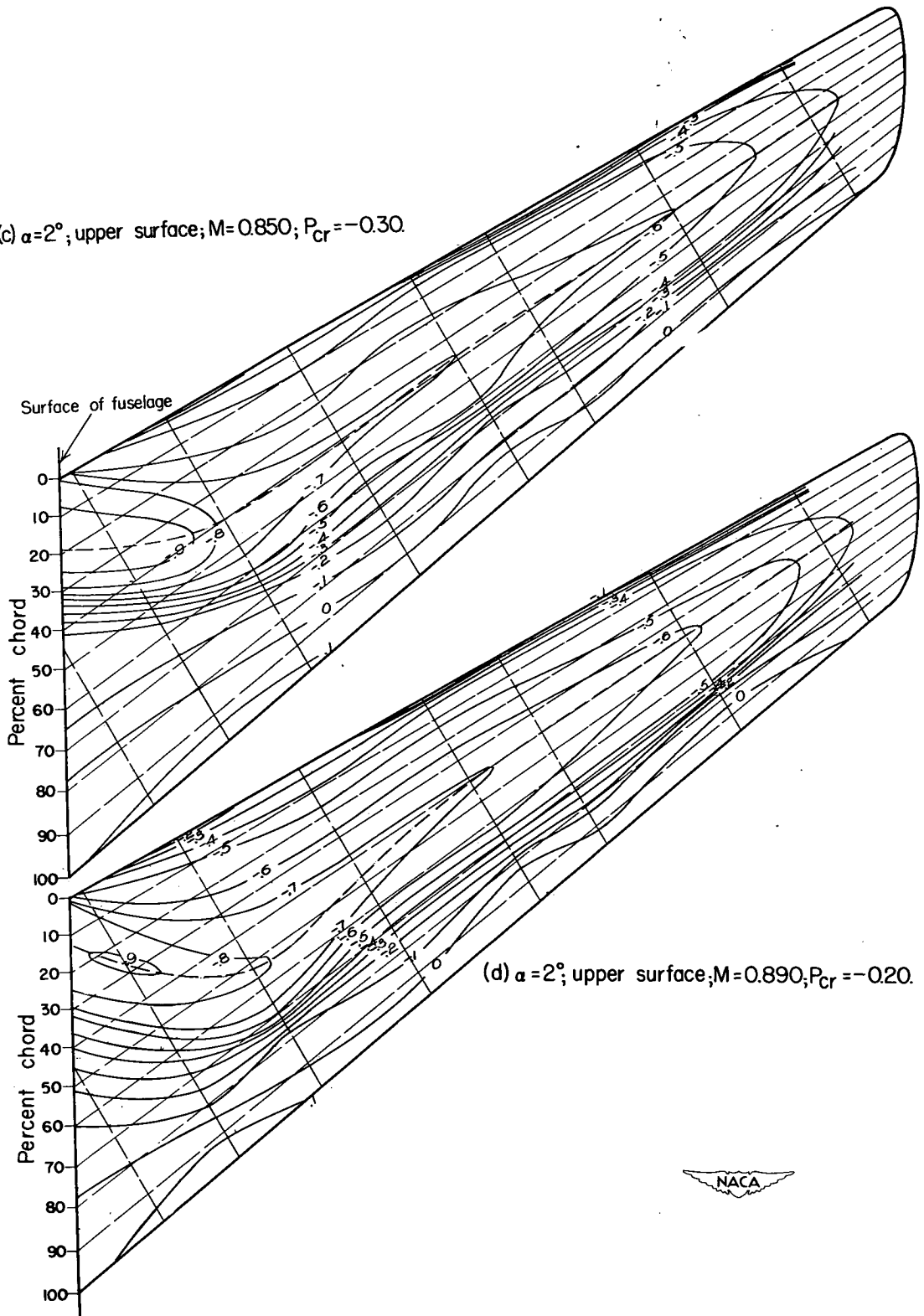


Figure 4.- Equal pressure-coefficient contours.  $\Lambda = -30^\circ$ .

(c)  $\alpha=2^\circ$ ; upper surface;  $M=0.850$ ;  $P_{Cr}=-0.30$ .



(d)  $\alpha=2^\circ$ ; upper surface;  $M=0.890$ ;  $P_{Cr}=-0.20$ .



Figure 4.- Continued.

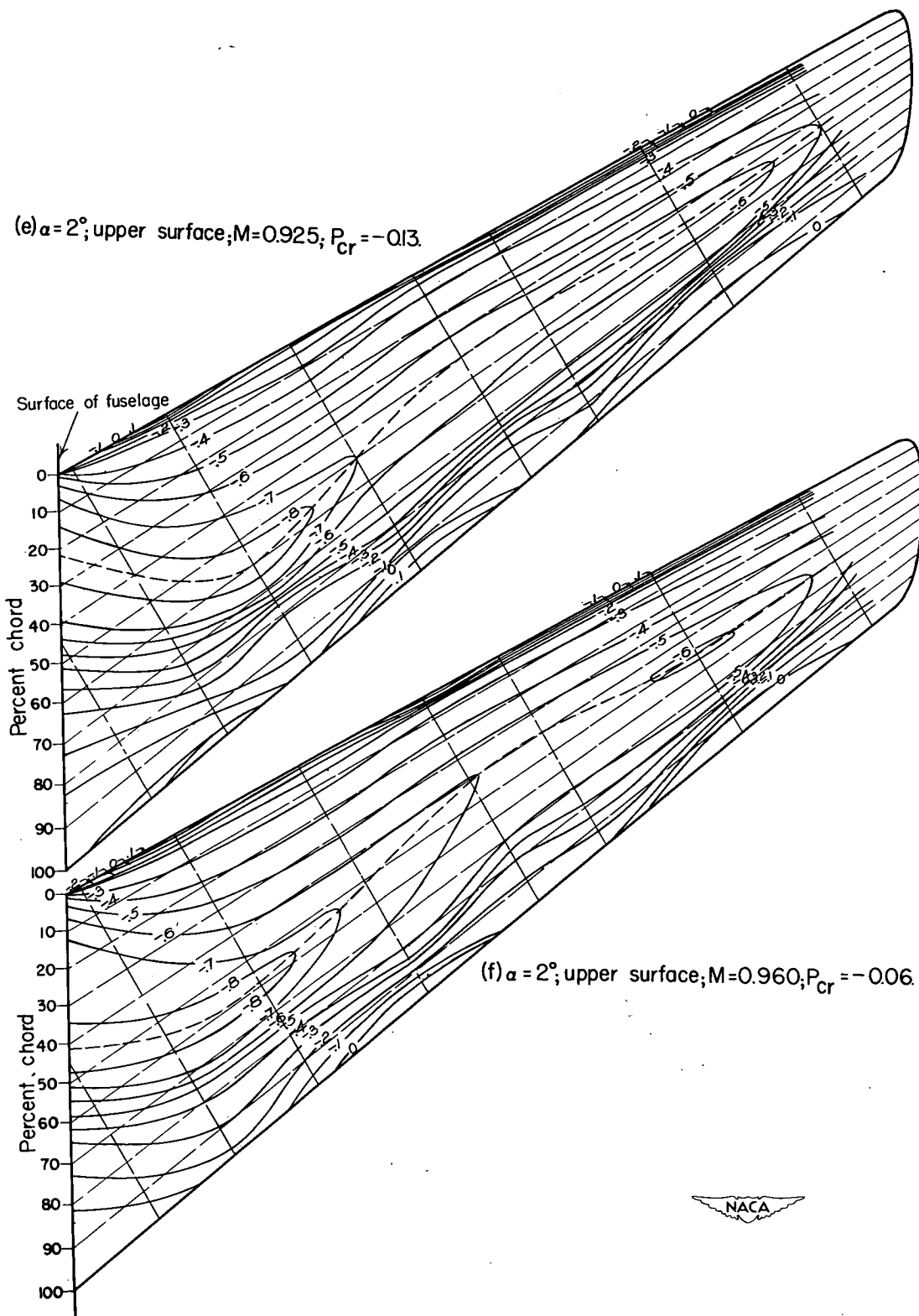


Figure 4.- Continued.

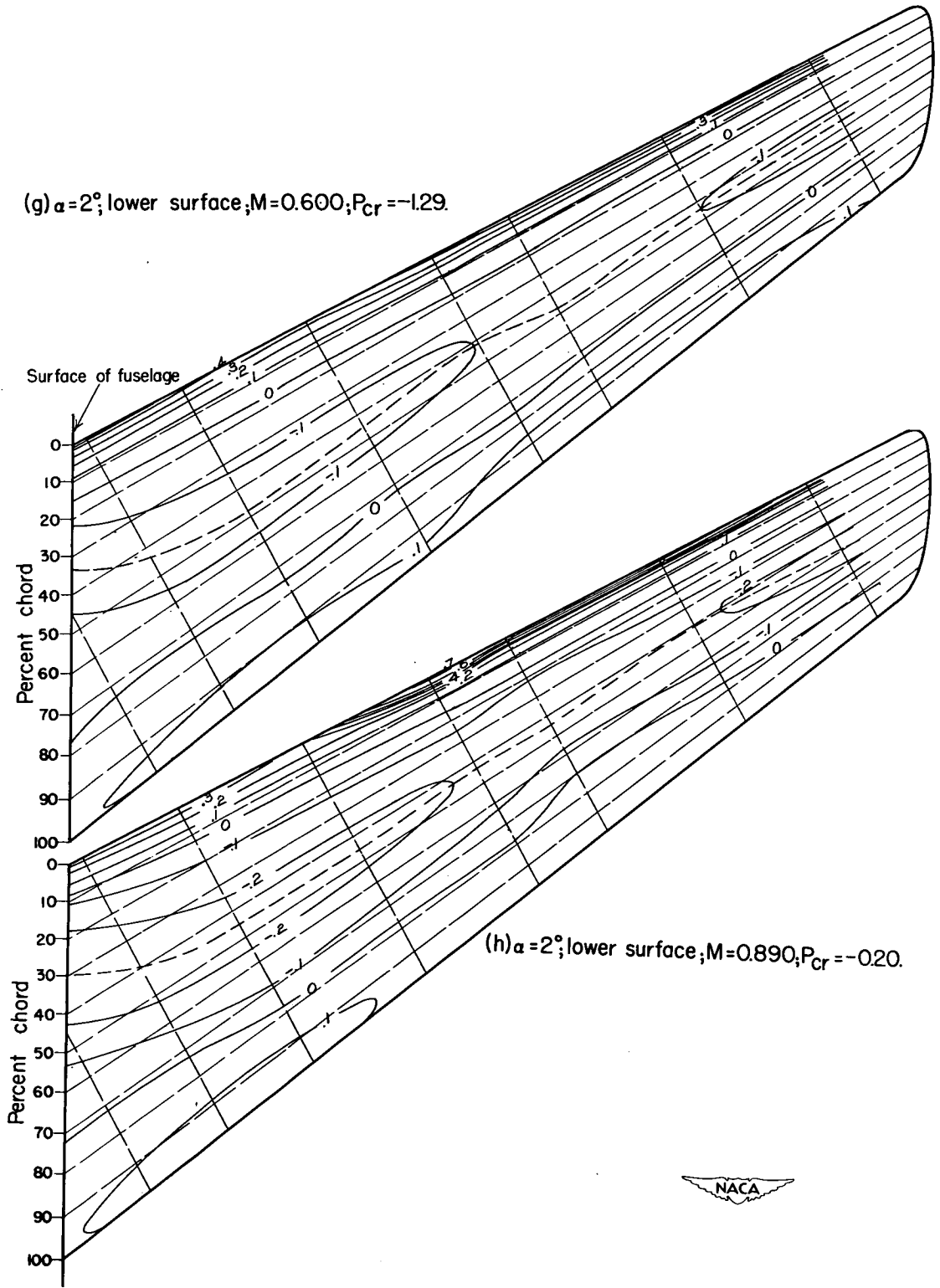


Figure 4.- Continued.

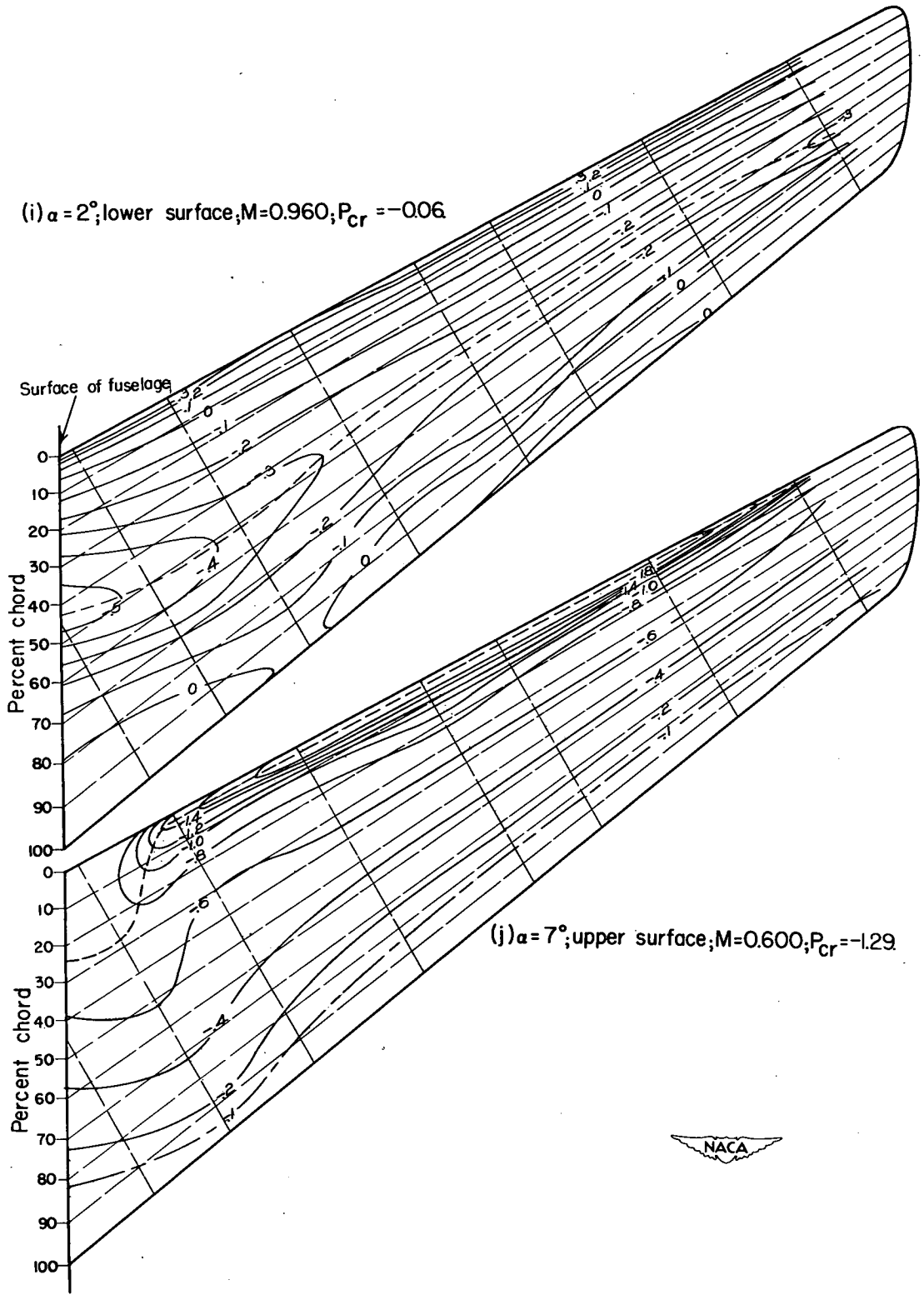


Figure 4.- Continued.

(k)  $\alpha = 7^\circ$ ; upper surface;  $M = 0.850$ ;  $P_{Cr} = -0.30$ .

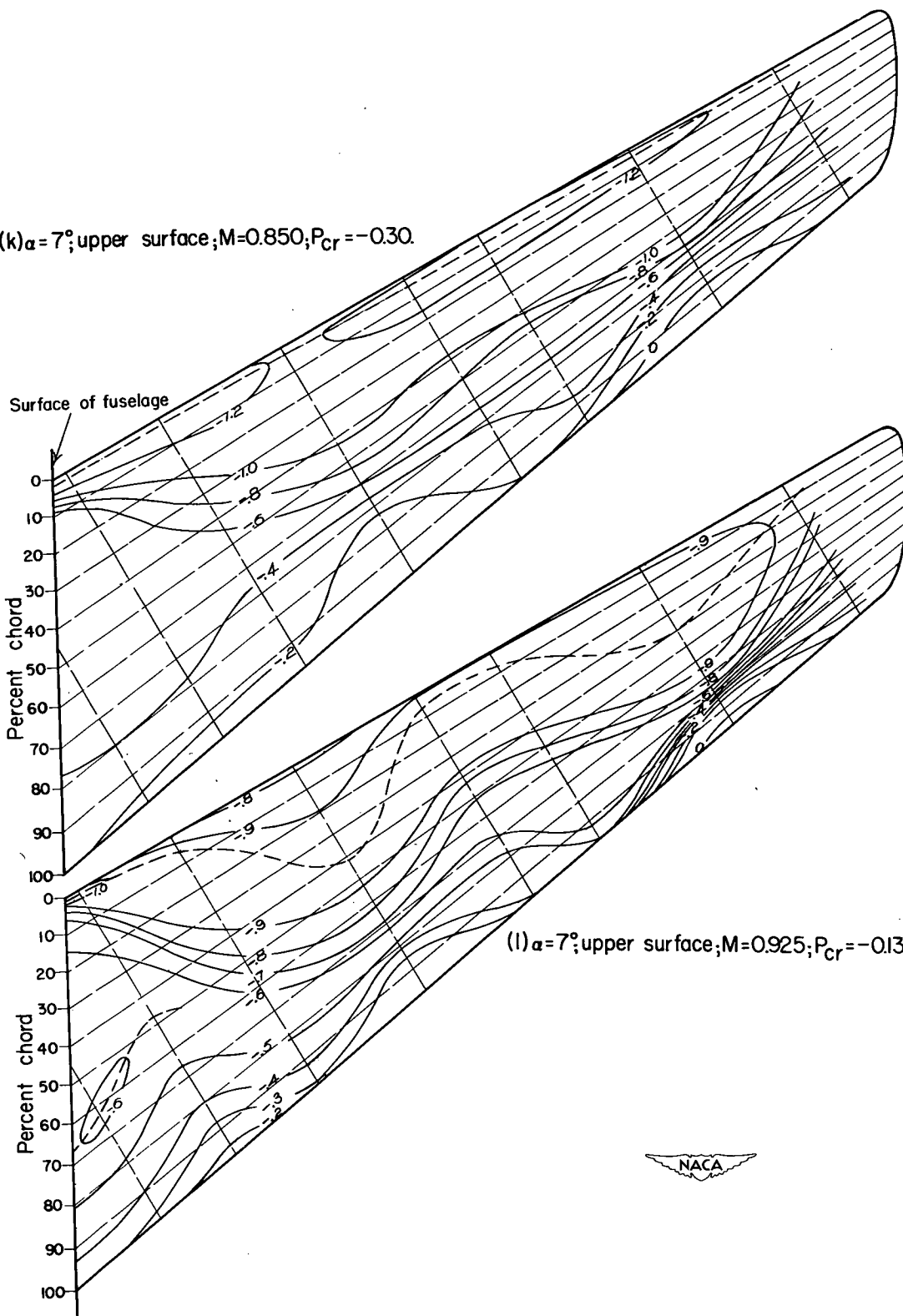


Figure 4.- Continued.

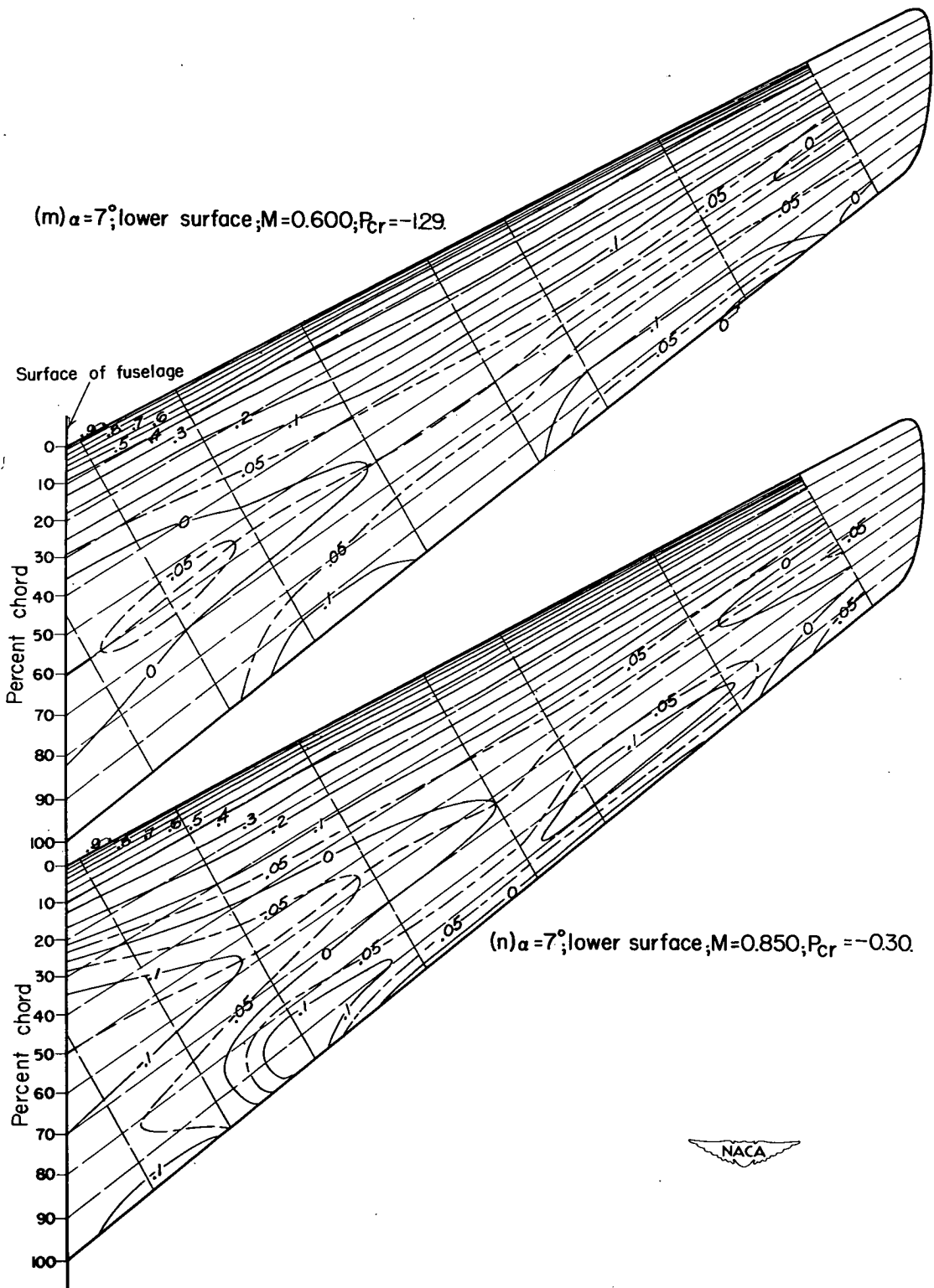


Figure 4.- Concluded.



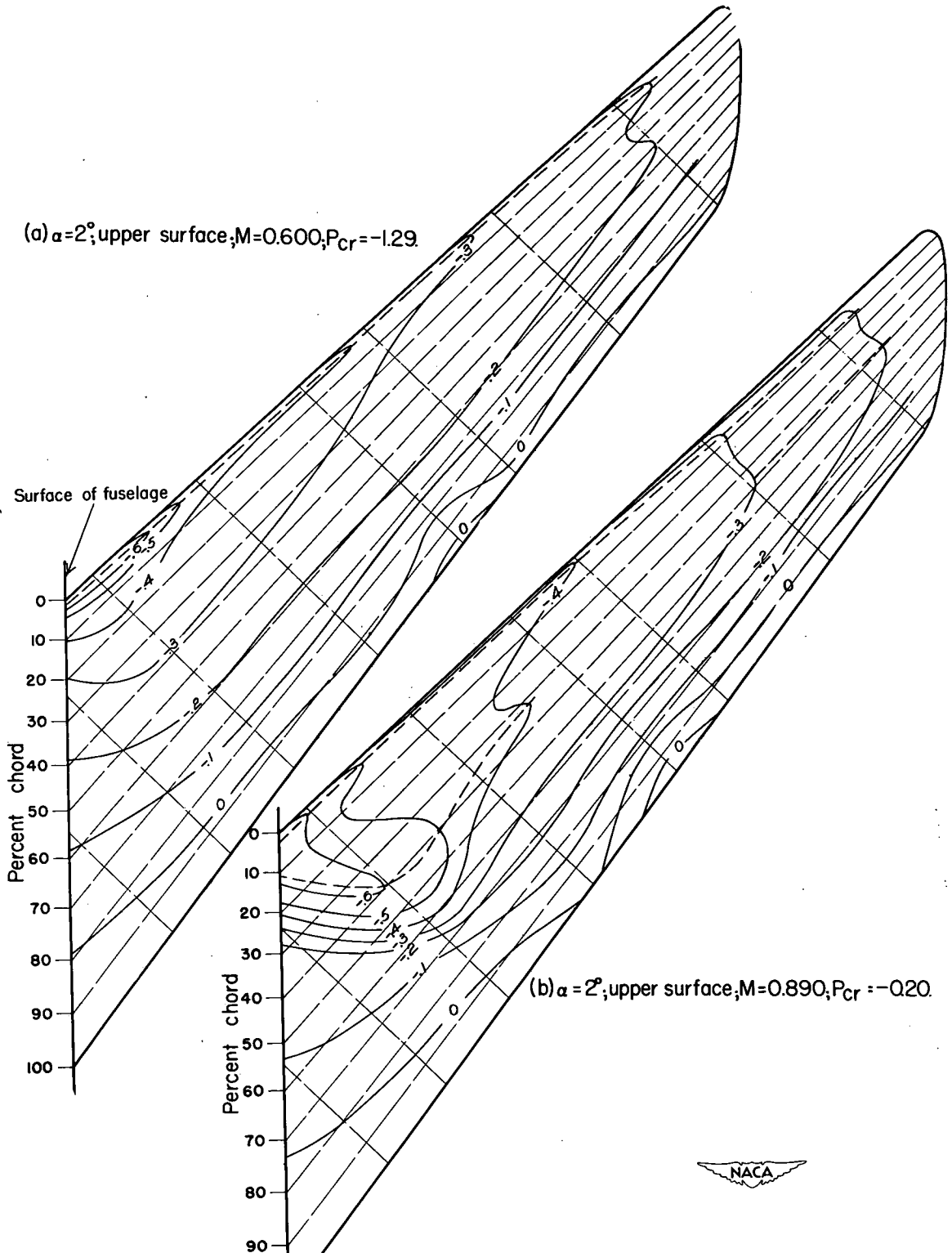


Figure 5.- Equal pressure-coefficient contours.  $\Lambda = -45^\circ$ .

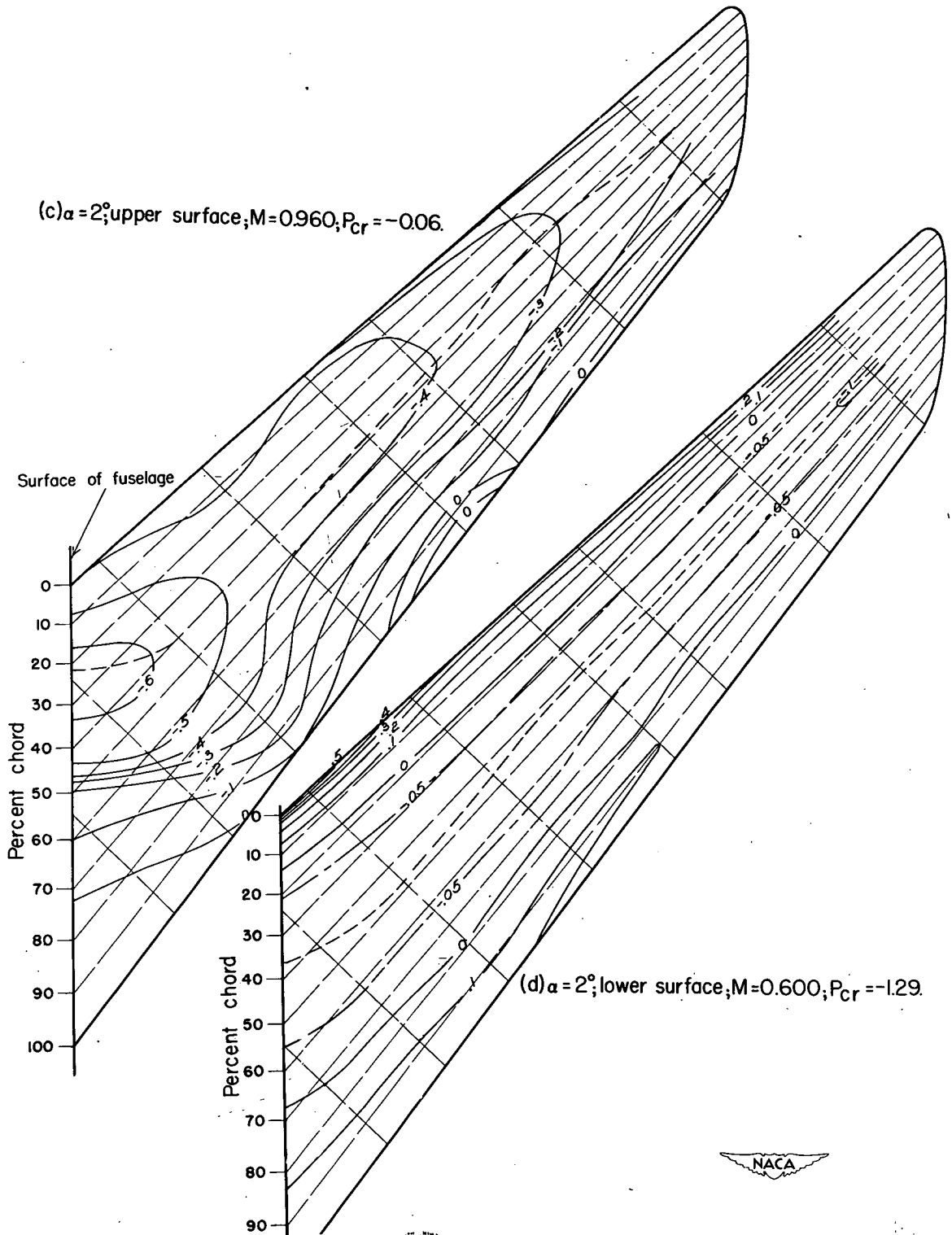
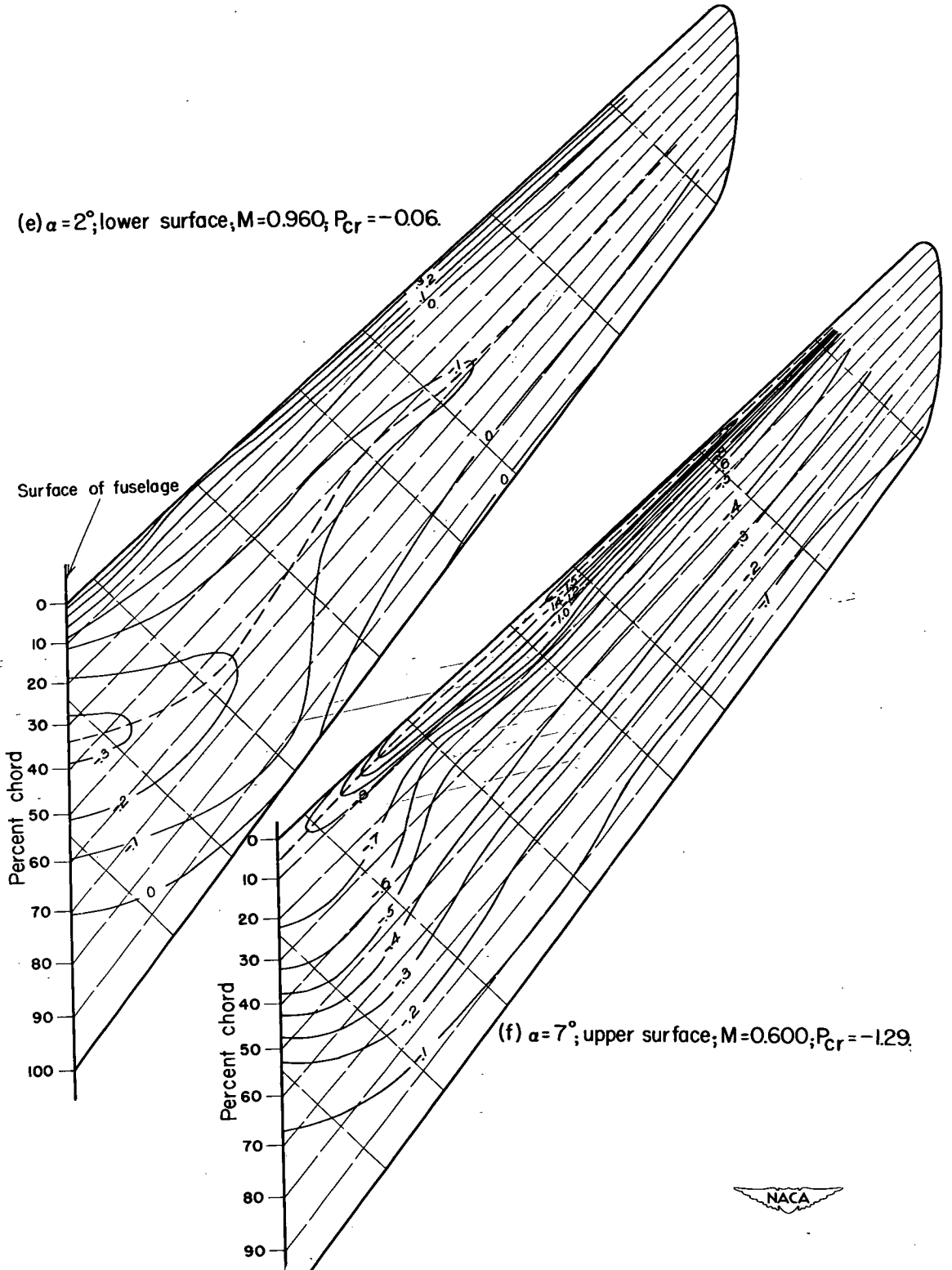


Figure 5.- Continued.

(e)  $\alpha = 2^\circ$ ; lower surface,  $M = 0.960$ ,  $P_{Cr} = -0.06$ .



(f)  $\alpha = 7^\circ$ ; upper surface,  $M = 0.600$ ,  $P_{Cr} = -1.29$ .



Figure 5.- Continued.

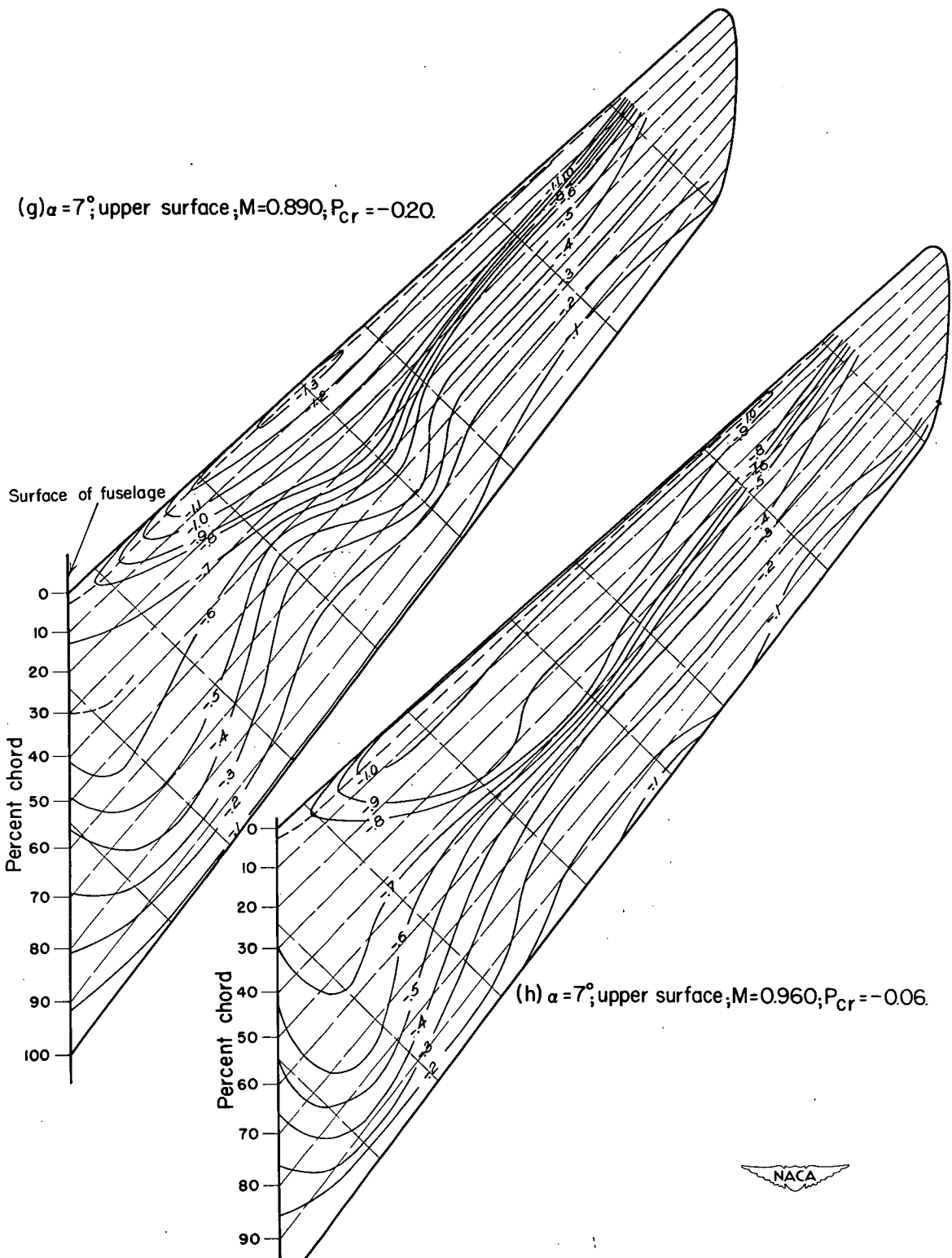
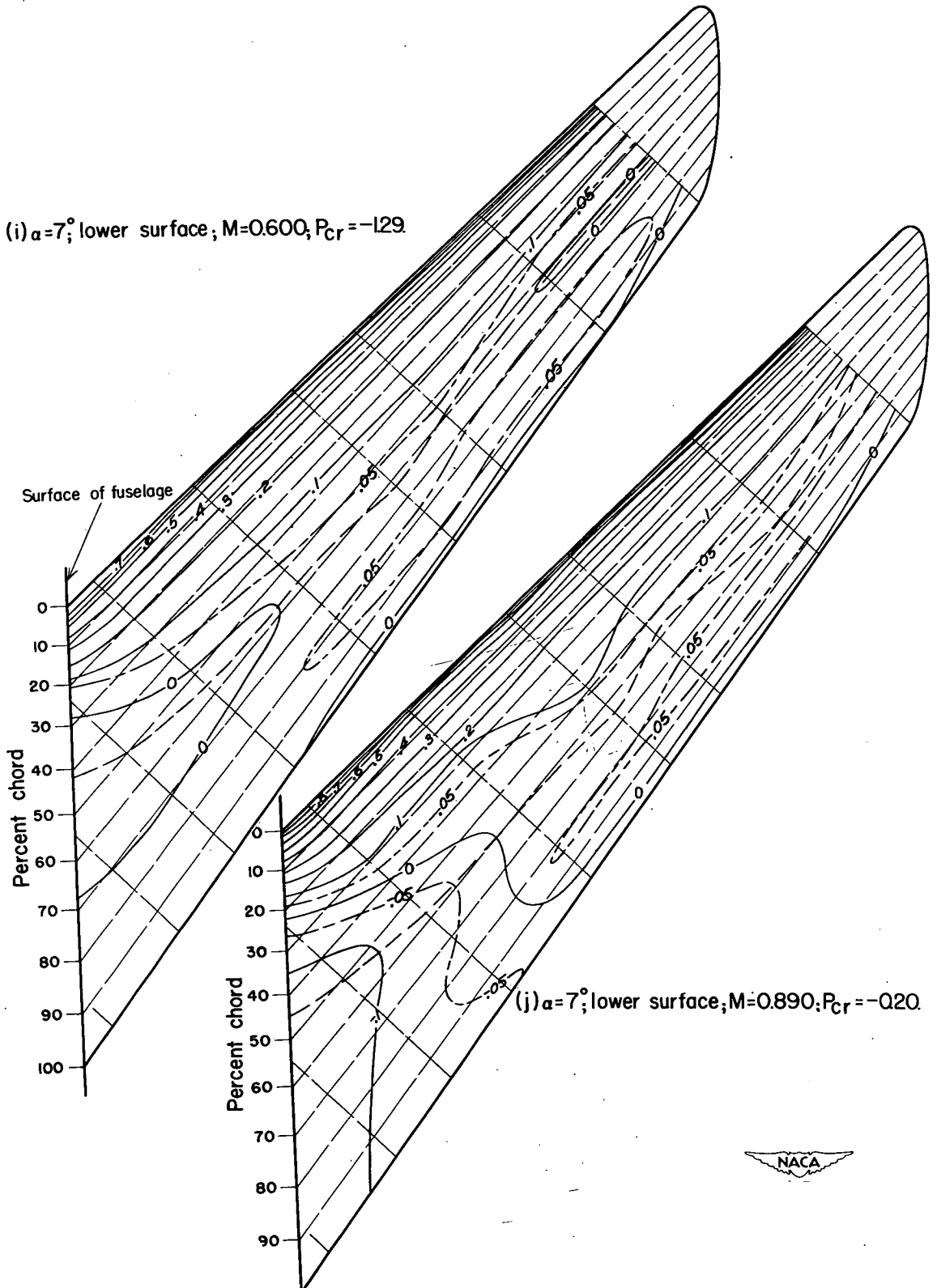


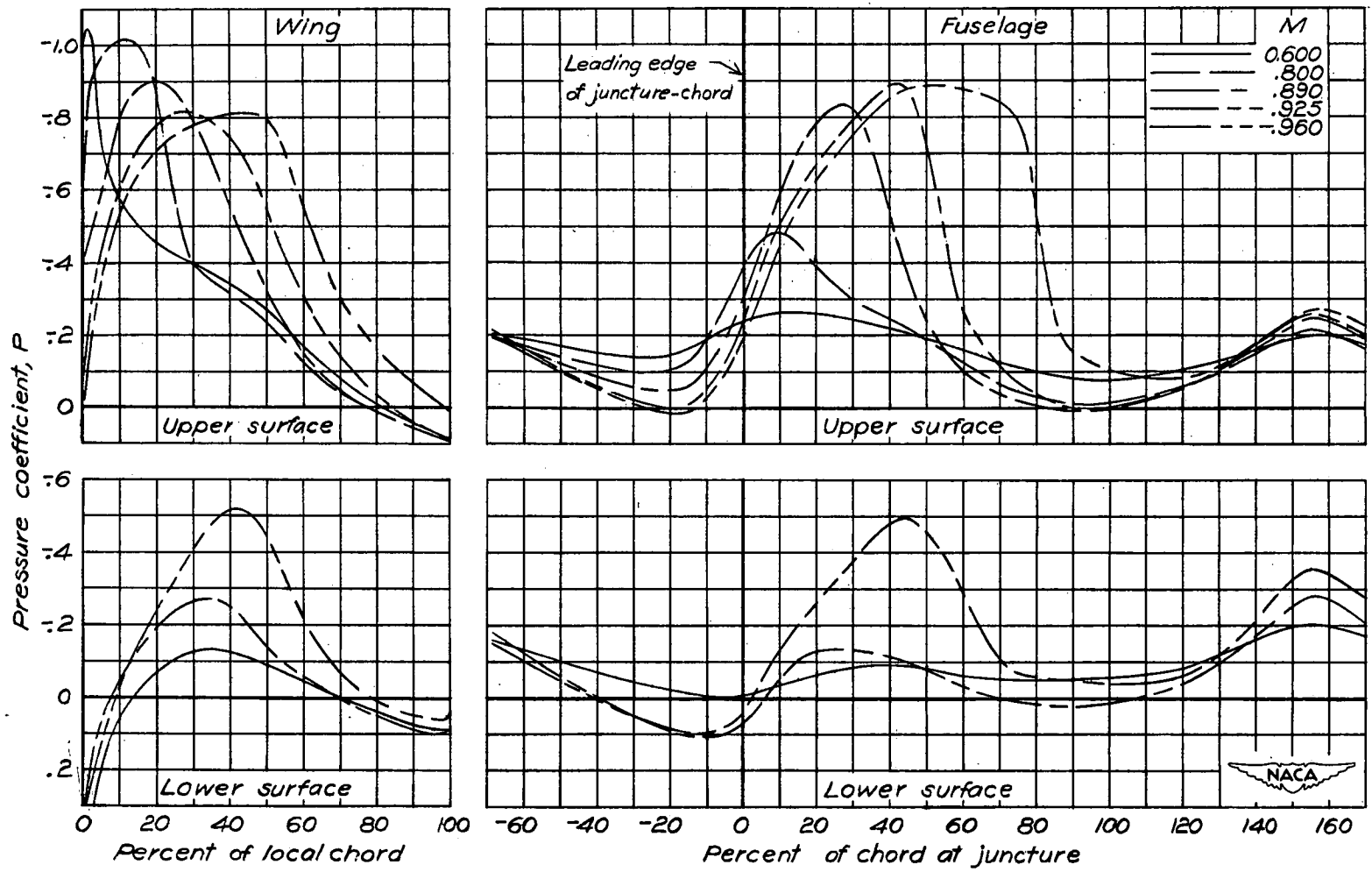
Figure 5.- Continued.

(i)  $\alpha=7^\circ$ ; lower surface;  $M=0.600$ ;  $P_{Cr}=-129$



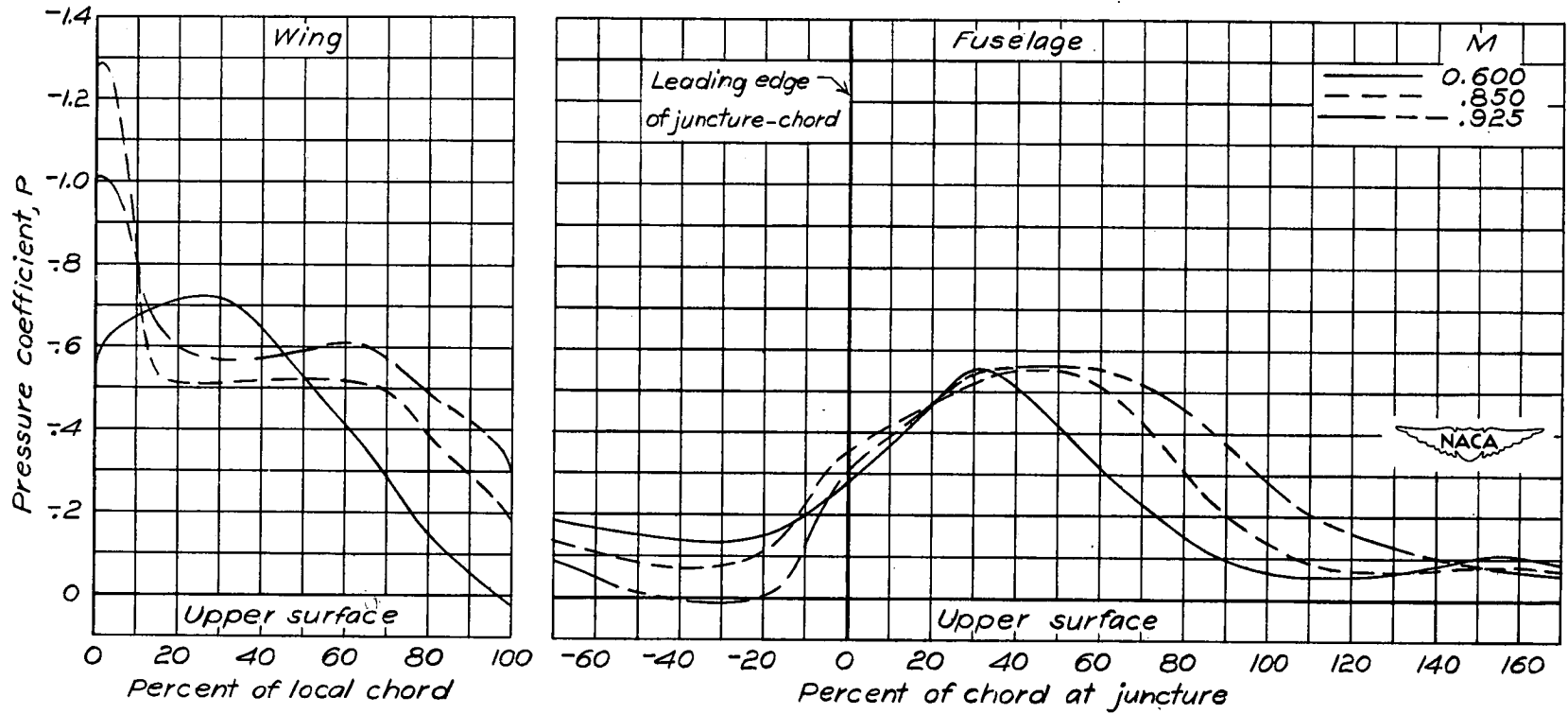
(j)  $\alpha=7^\circ$ ; lower surface;  $M=0.890$ ;  $P_{Cr}=-020$

Figure 5.- Concluded.



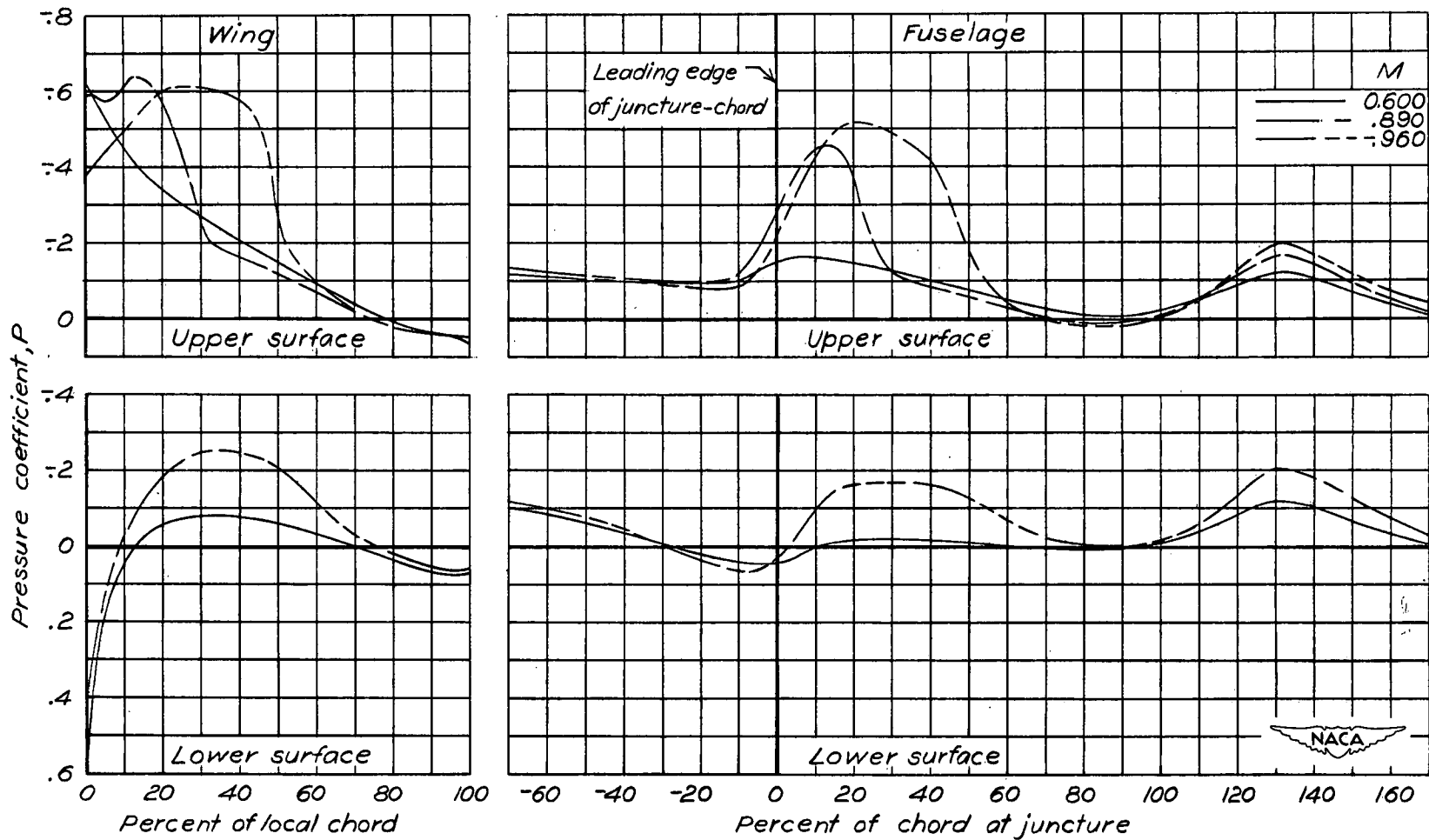
(a)  $\alpha = 2^\circ$ .

Figure 6.- Chordwise pressure distributions near wing-fuselage juncture.  
 $\Lambda = -30^\circ$ .



(b)  $\alpha = 7^\circ$ .

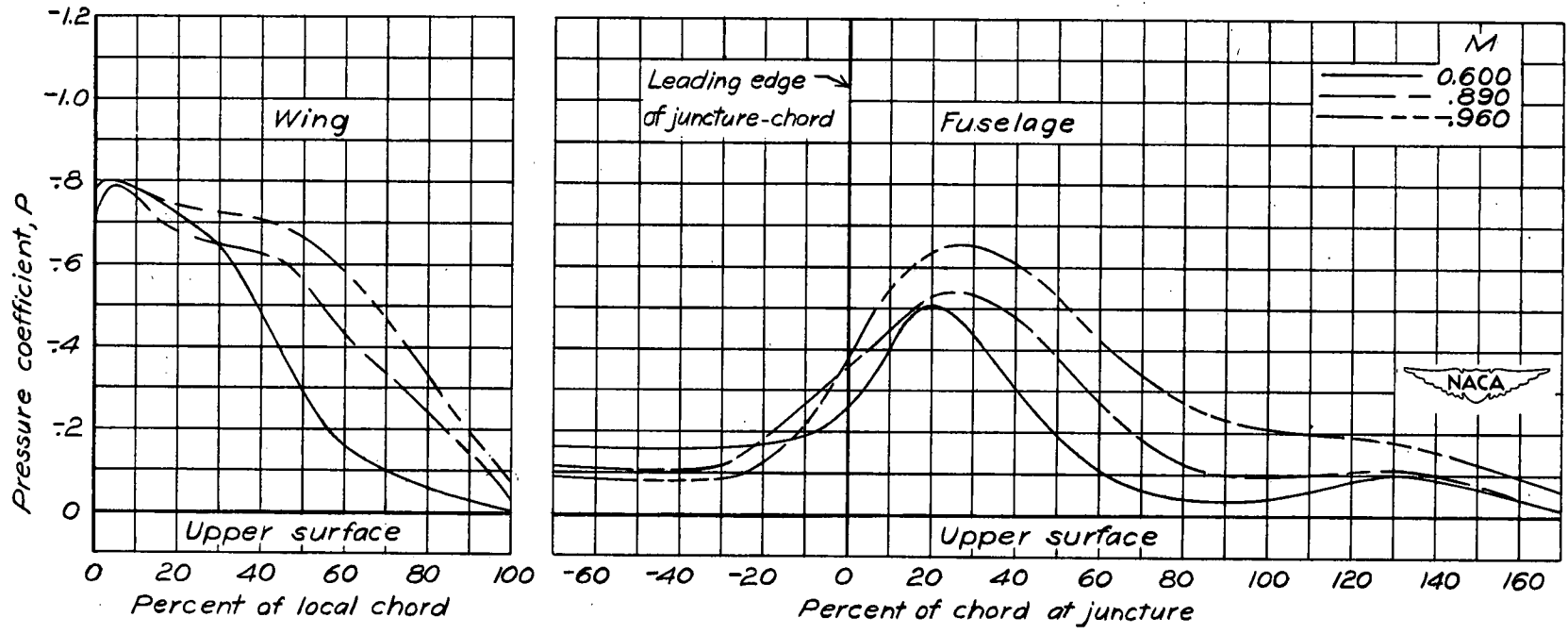
Figure 6.- Concluded.  $\Lambda = - 30^\circ$ .



(a)  $\alpha = 2^\circ$ .

Figure 7.- Chordwise pressure distributions near wing-fuselage juncture.  
 $\Lambda = -45^\circ$ .





(b)  $\alpha = 7^\circ$ .

Figure 7.- Concluded.  $\Lambda = -45^\circ$ .

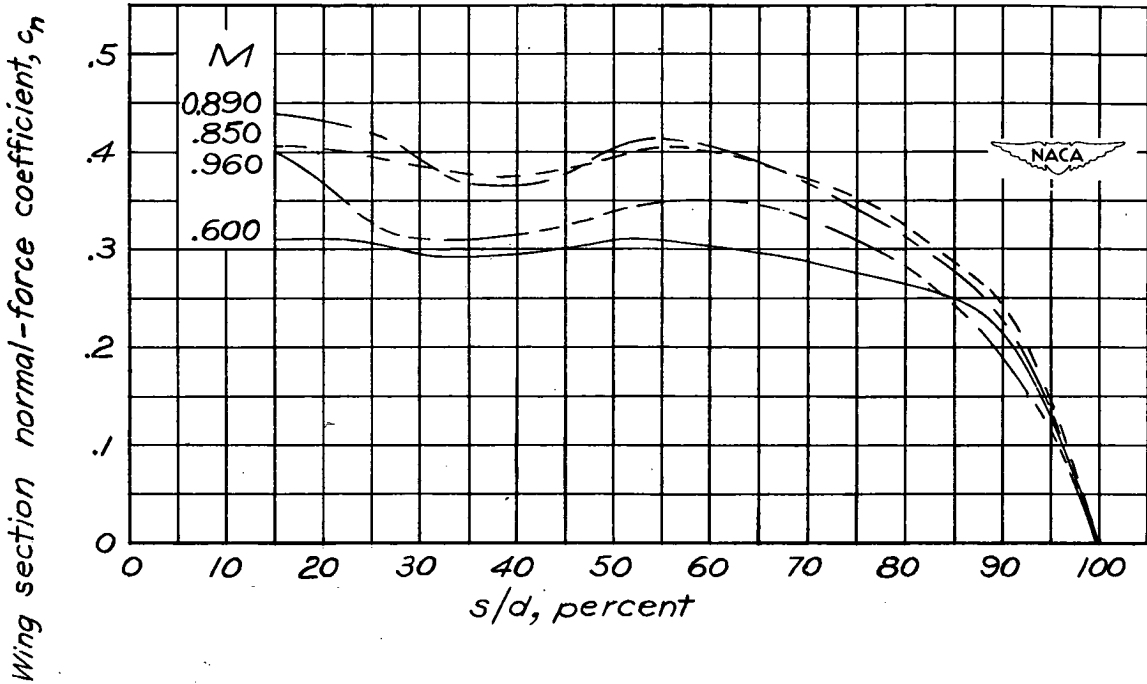


Figure 8.- Spanwise variations of wing-section normal-force coefficient for various Mach numbers.  $\Lambda = -30^\circ$ ;  $\alpha = 2^\circ$ .

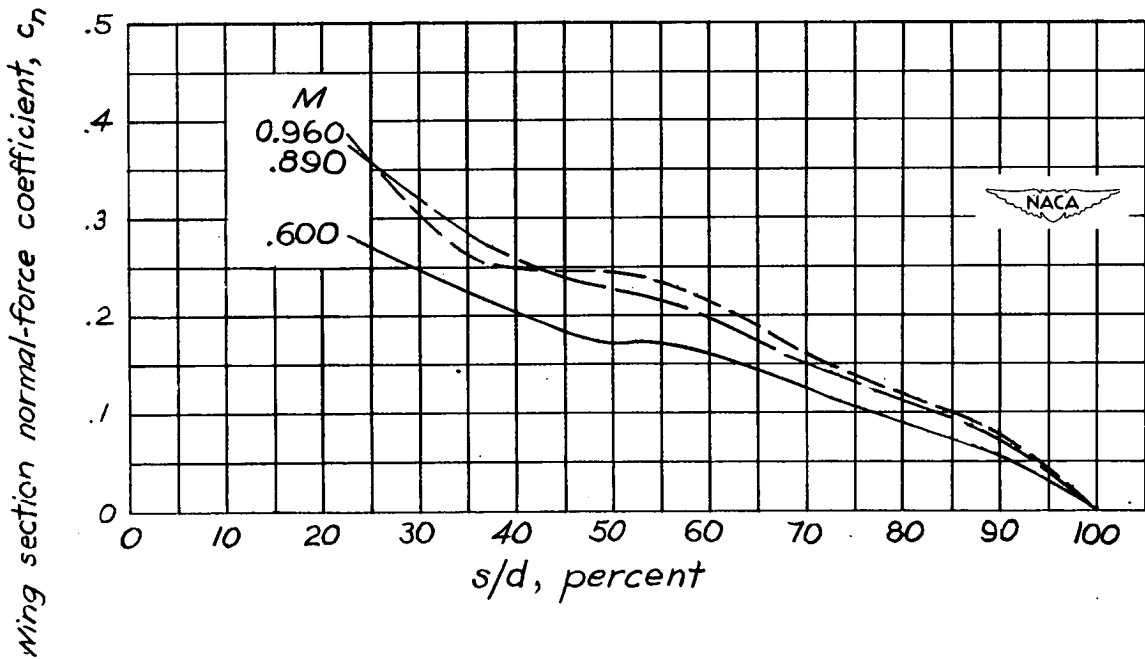
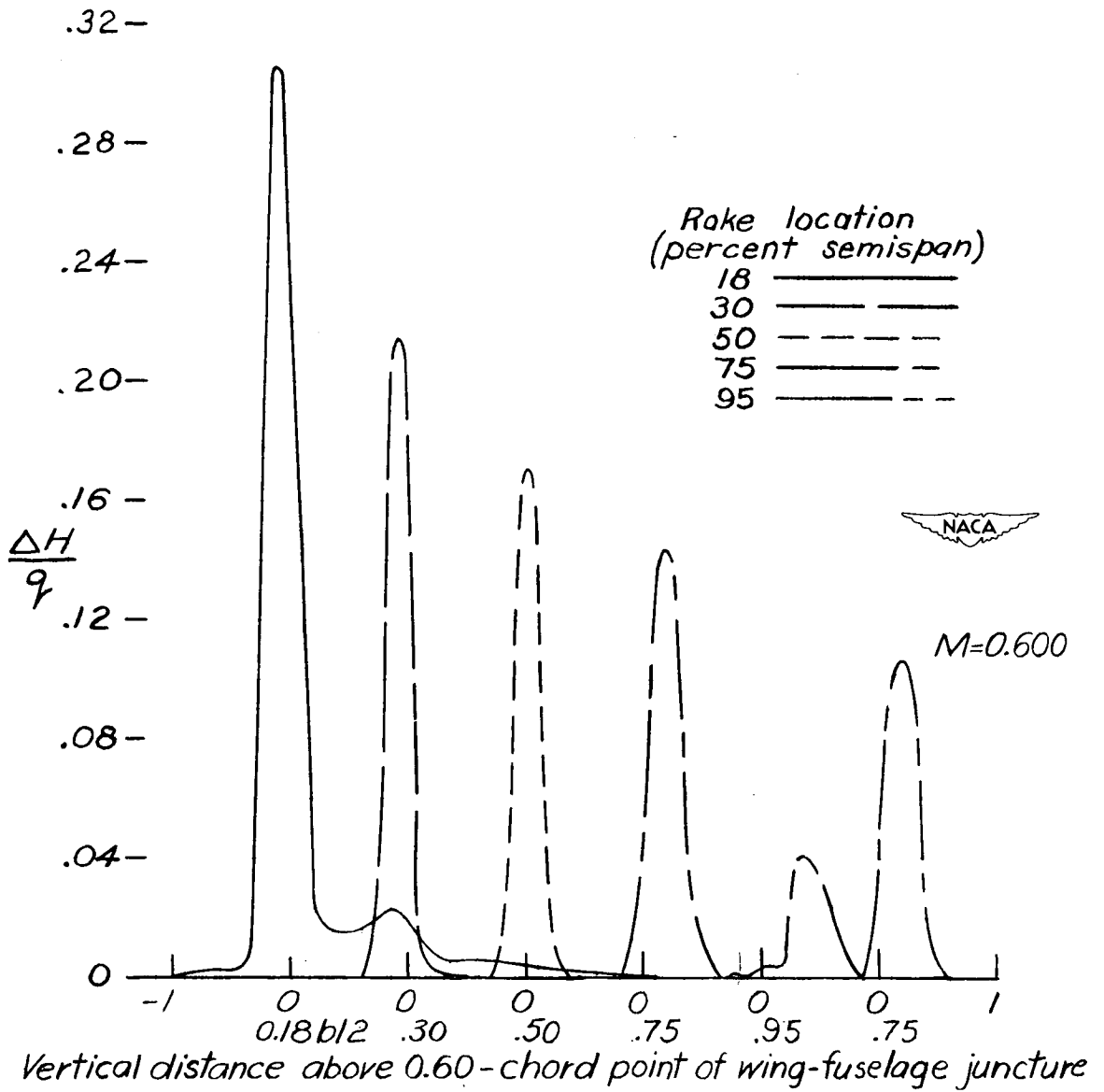
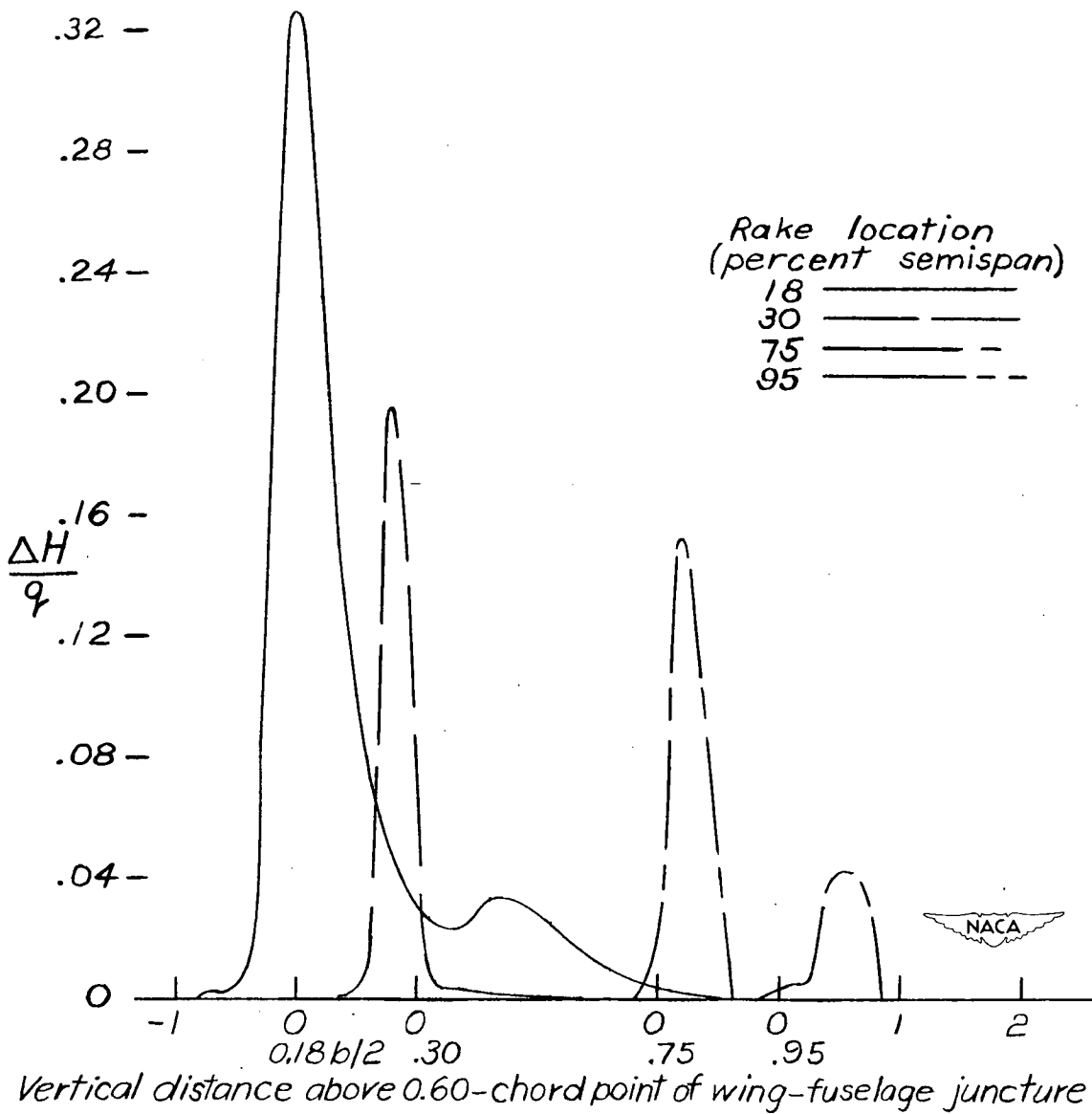


Figure 9.- Spanwise variations of wing-section normal-force coefficient for various Mach numbers.  $\Lambda = -45^\circ$ ;  $\alpha = 2^\circ$ .



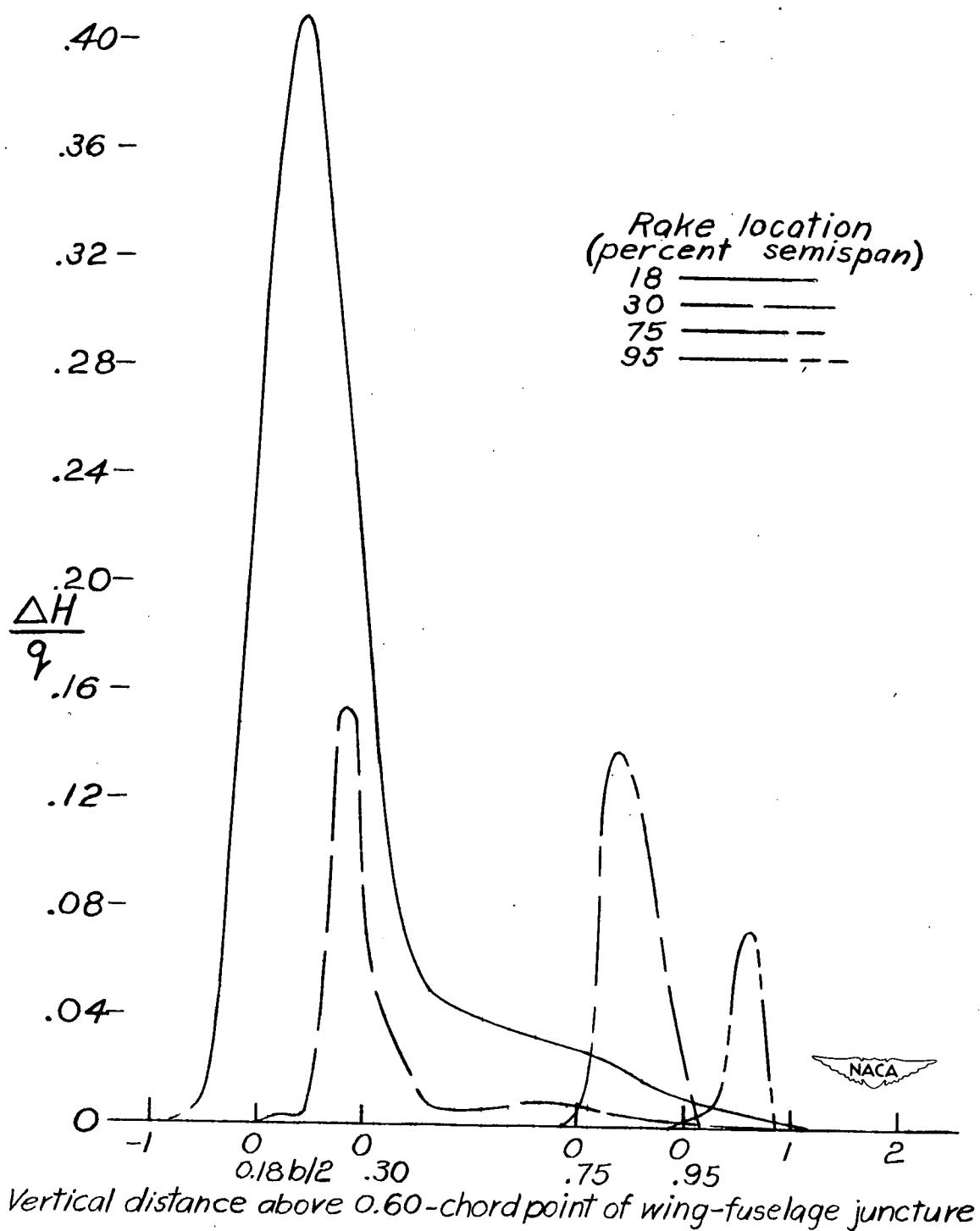
(a)  $\alpha = 2^\circ$ ;  $M = 0.800$ .

Figure 10.- Wake profiles at various spanwise vertical survey positions.  
 $\Lambda = -30^\circ$ .



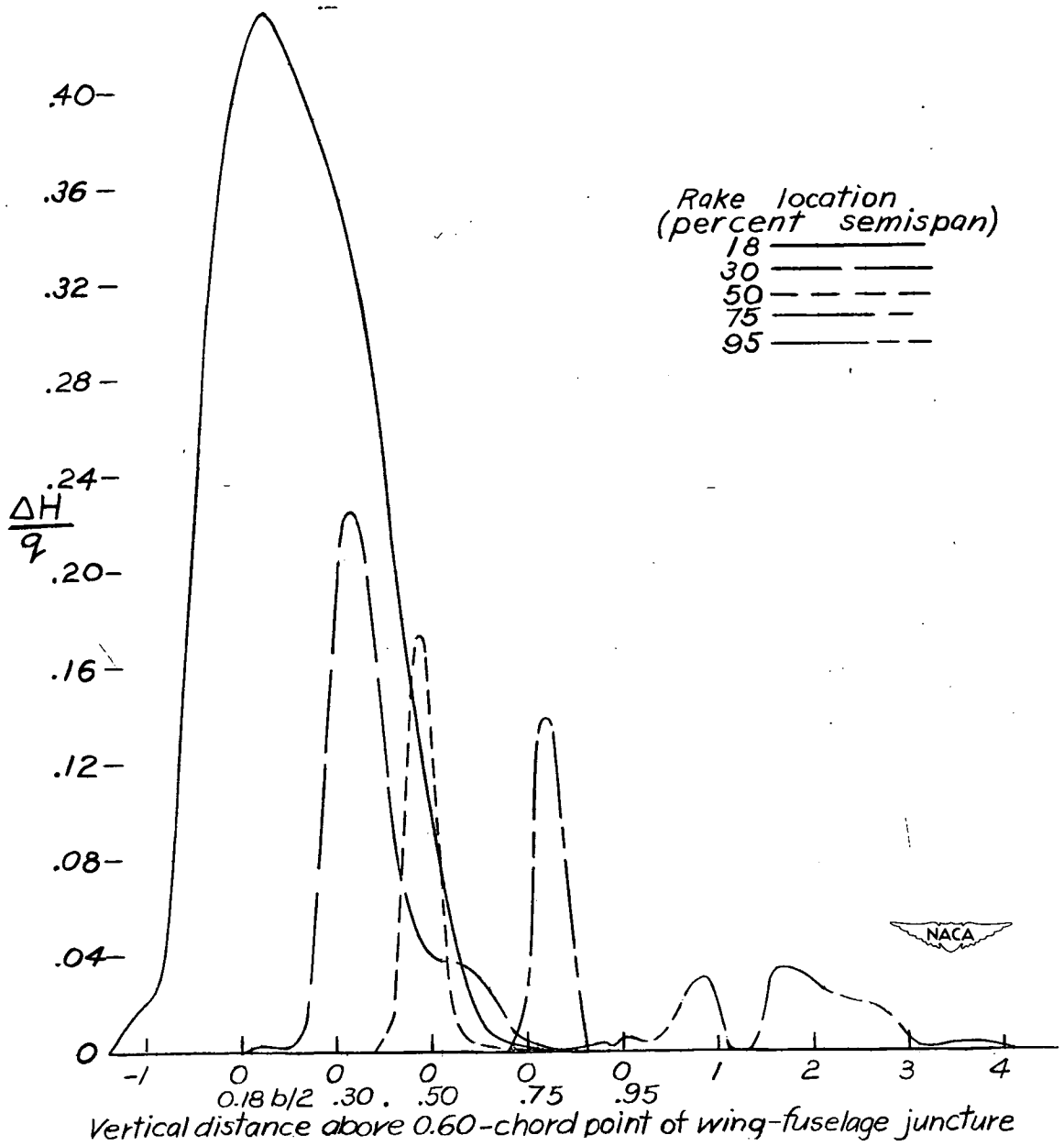
(b)  $\alpha = 2^\circ$ ;  $M = 0.850$ .

Figure 10.- Continued.  $\Lambda = -30^\circ$ .



(c)  $\alpha = 2^\circ$ ;  $M = 0.890$ .

Figure 10.- Continued.  $\Lambda = -30^\circ$ .



(d)  $\alpha = 5^\circ$ ;  $M = 0.800$ .

Figure 10.- Concluded.  $\Lambda = -30^\circ$ .

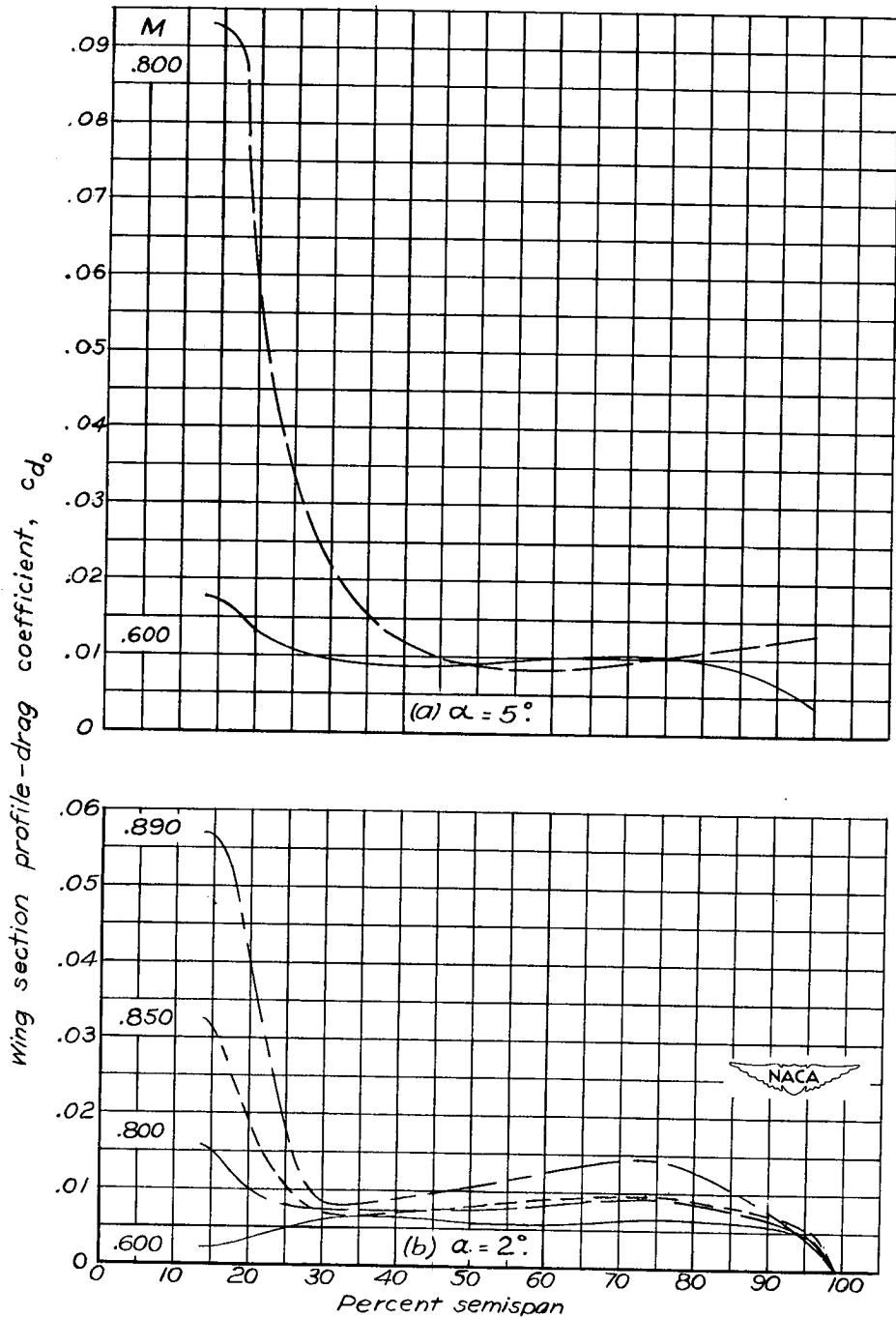


Figure 11.- Spanwise variations of wing-section profile-drag coefficient for various Mach numbers.  $\Lambda = -30^\circ$ .

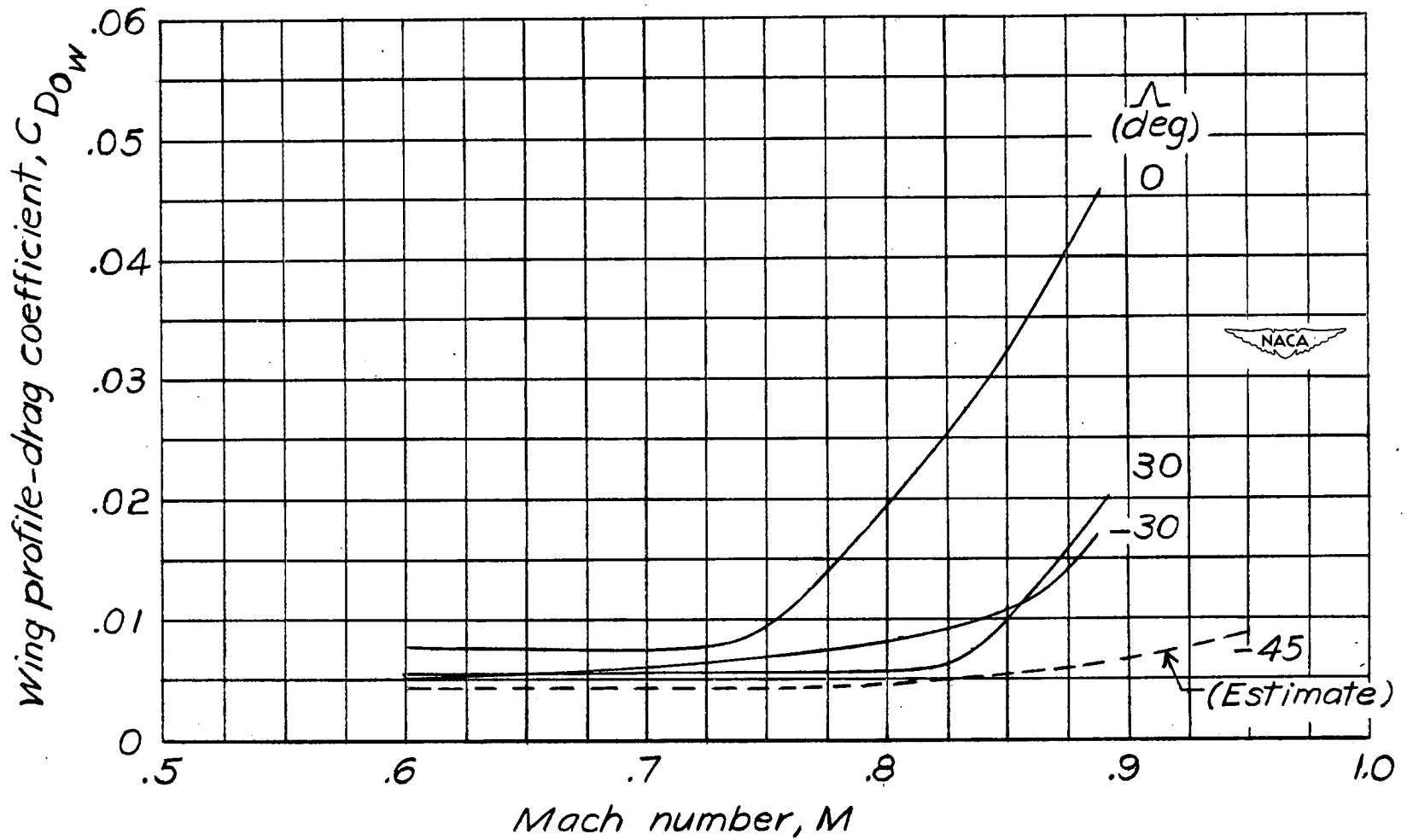
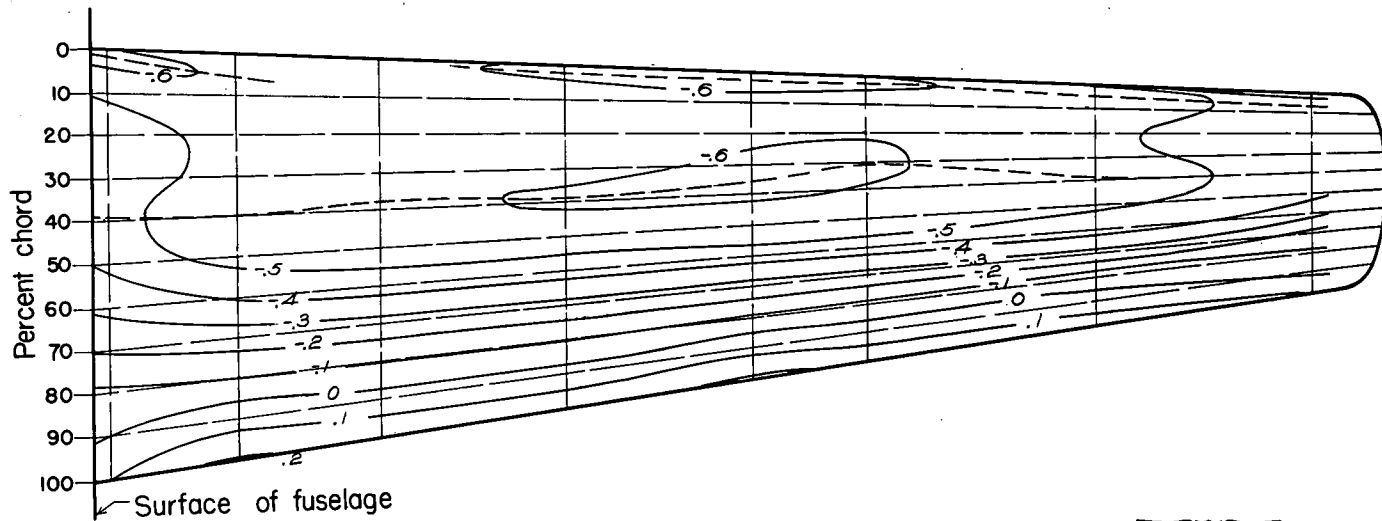


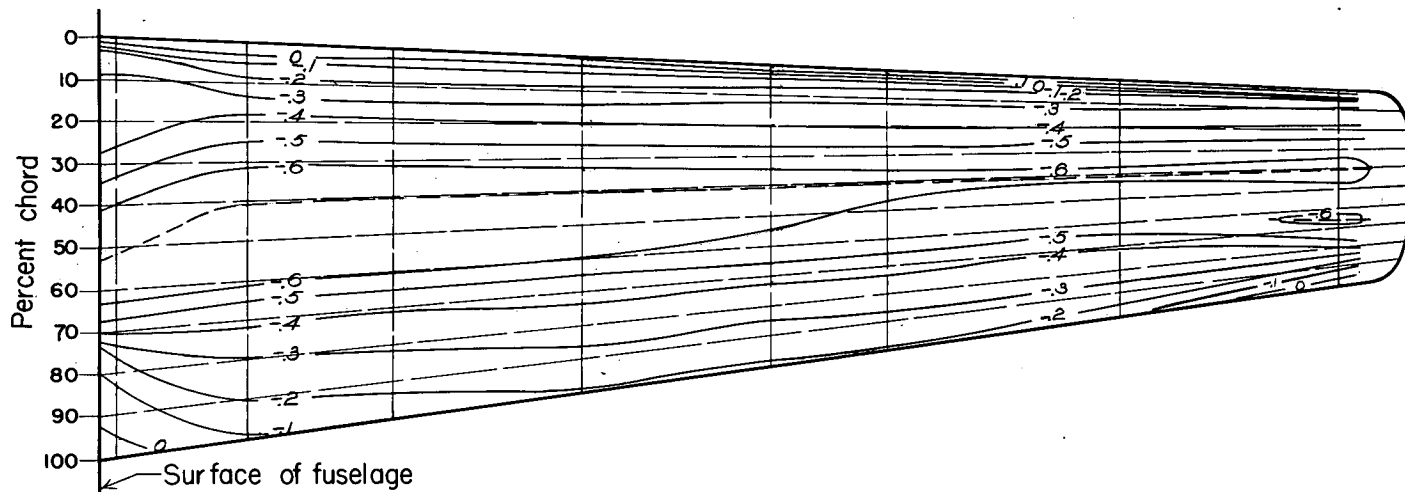
Figure 12.- Variations of wing profile-drag coefficients with Mach number for various amounts of sweepforward.  $\alpha = 2^\circ$ .





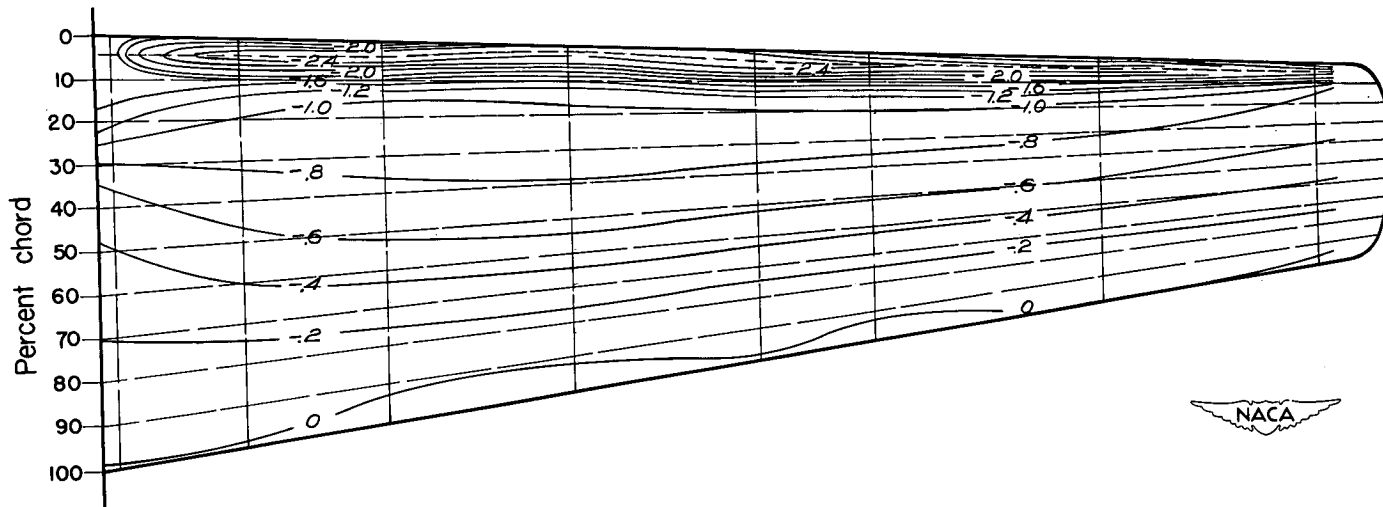
(a)  $\alpha = 2^\circ$ ; upper surface;  $M = 0.60$ ;  $P_{cr} = -1.29$ .

Figure 13.- Equal pressure-coefficient contours,  $\Lambda = 0^\circ$ .



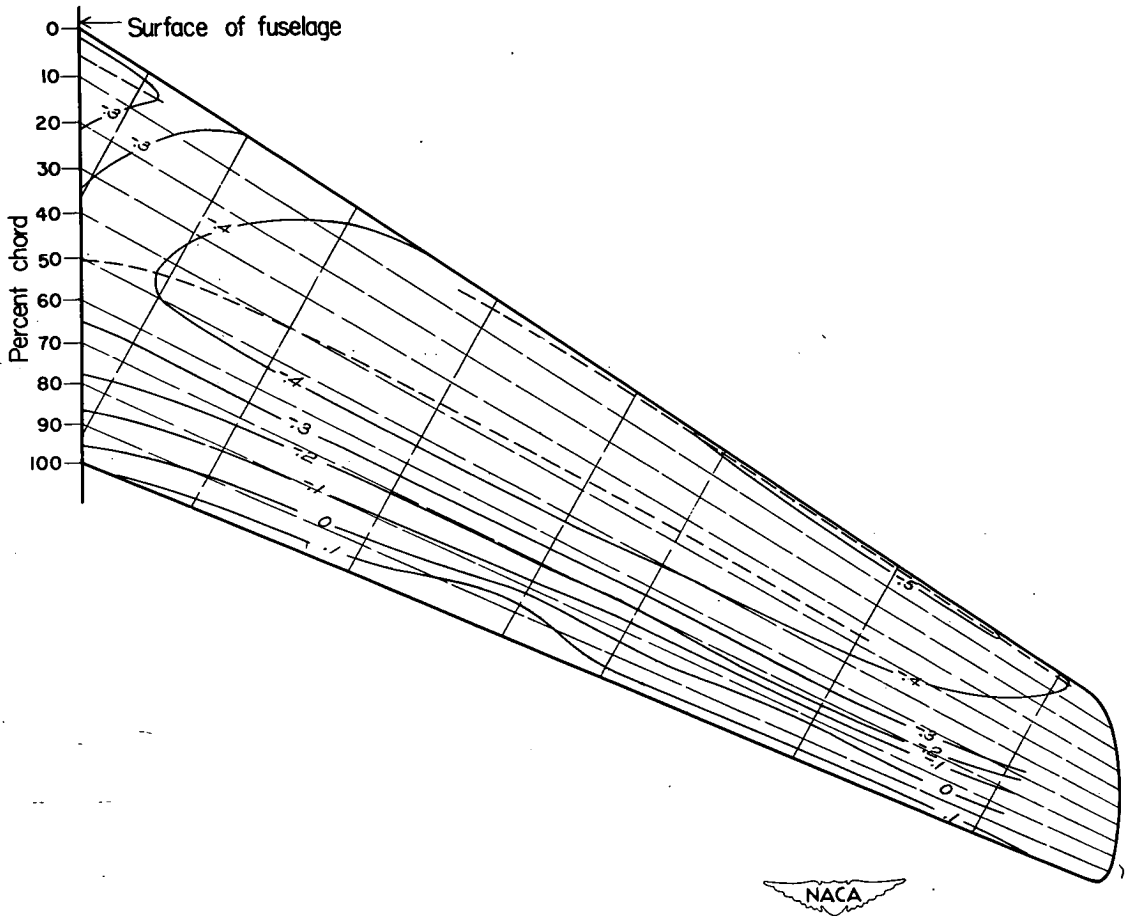
(b)  $\alpha = 2^\circ$ ; upper surface;  $M = 0.89$ ;  $P_{cr} = -0.20$ .

Figure 13.- Continued.



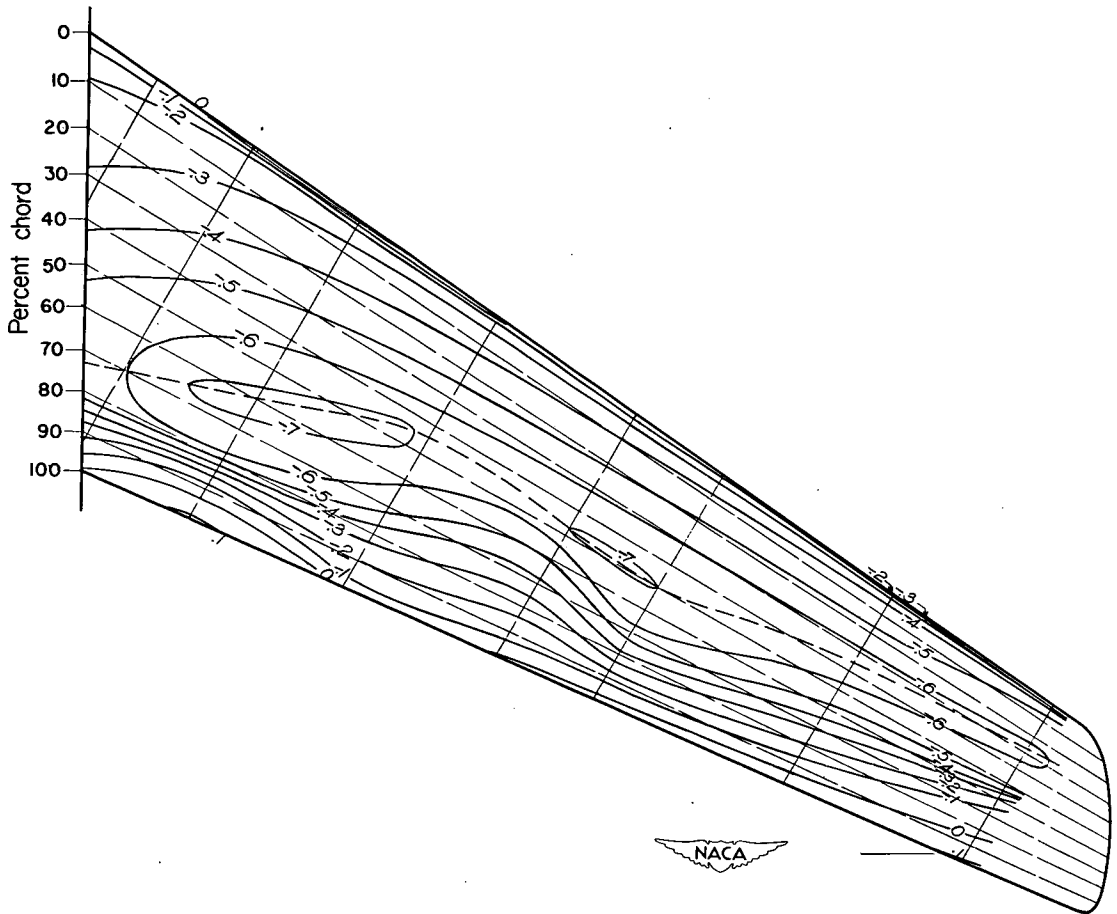
(c)  $\alpha = 7^\circ$ ; upper surface;  $M = 0.60$ ;  $P_{cr} = -1.29$ .

Figure 13.- Concluded.



(a)  $\alpha = 2^\circ$ ; upper surface;  $M = 0.60$ ;  $P_{cr} = -1.29$ .

Figure 14.- Equal pressure-coefficient contours,  $\Lambda = 30^\circ$ .



(b)  $\alpha = 2^\circ$ ; upper surface;  $M = 0.89$ ;  $P_{cr} = -0.20$ .

Figure 14.- Concluded.

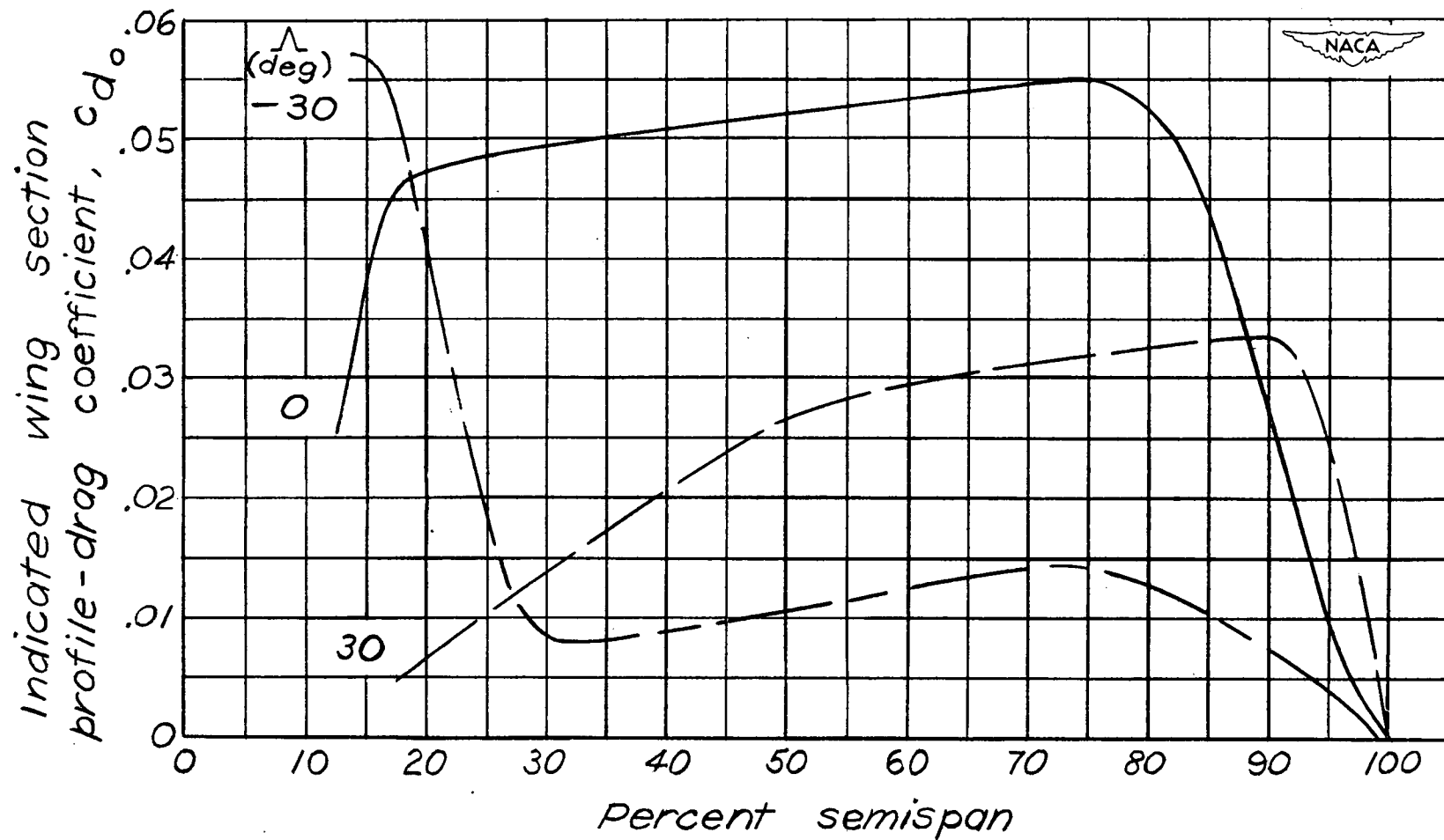


Figure 15.- Spanwise variations of indicated wing-section profile-drag coefficient for several angles of sweep;  $\alpha = 2^\circ$ ;  $M = 0.89$ .

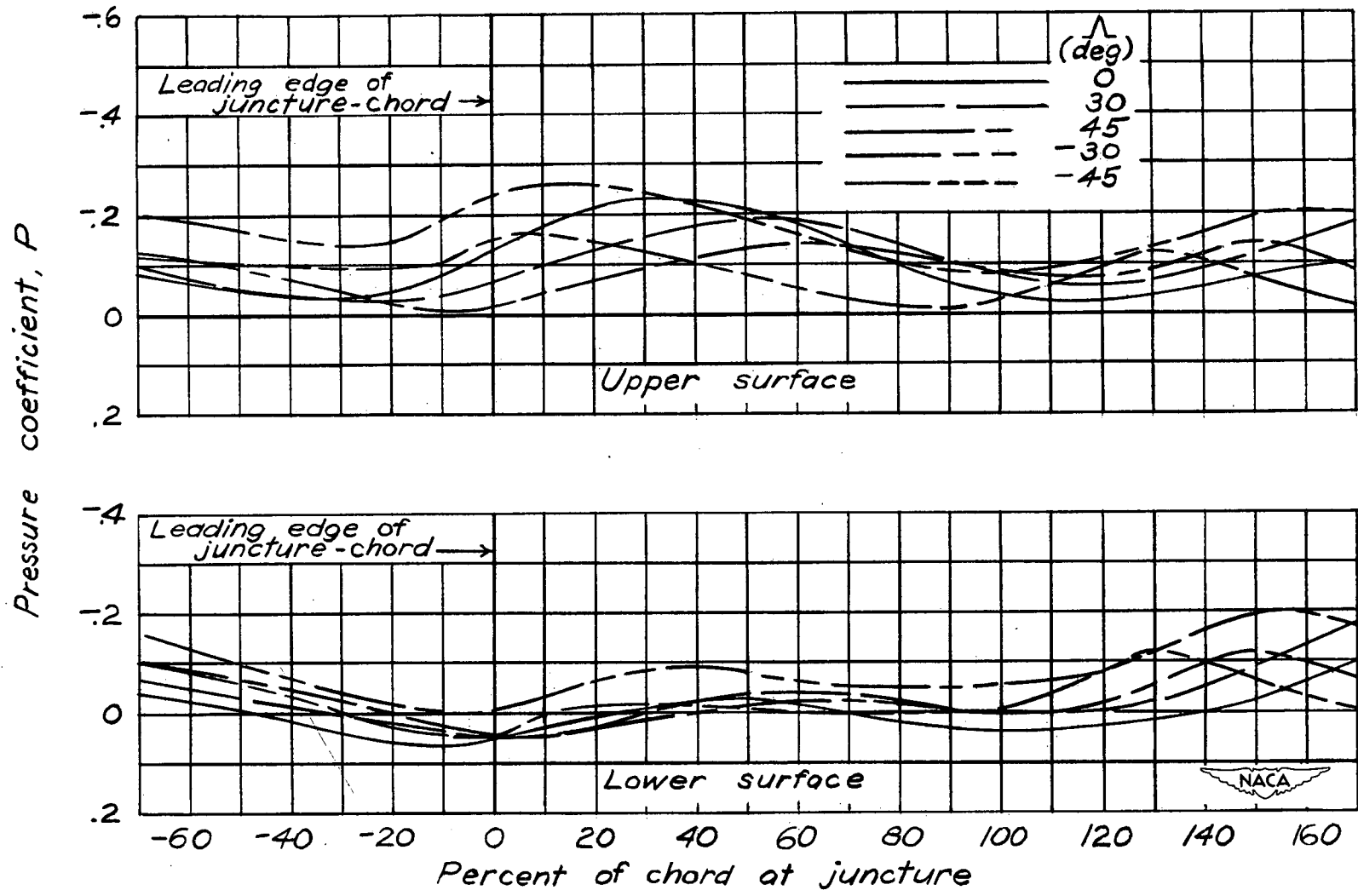


Figure 16.- Streamwise distributions of pressure coefficient on fuselage for various angles of sweepback and sweepforward;  $\alpha = 2^\circ$ ;  $M = 0.60$ .